Novel epidemiological model of gastrointestinal-nematode infection to assess grazing cattle resilience by integrating host growth, parasite, grass and environmental dynamics

J.A.N. Filipe [a*], I. Kyriazakis [b], C. McFarland [b], E.R. Morgan [b]

[a] Biomathematics & Statistics Scotland, Rowett Institute of Nutrition and Health, University of Aberdeen, AB25 2ZD, UK

[b] Institute for Global Food Security, Queen's University Belfast, Biological Sciences, 19, Chlorine Gardens, BT9 5DL, UK

***Corresponding author: Joao.Filipe@bioss.ac.uk**

HIGHLIGHTS

- Nematode control in cattle is complicated by drug resistance and climate change
- A model was developed to predict GIN epidemiology under varying conditions
- The model incorporates cattle growth, infection and immunity, grass availability, weather
- Predictions were validated against empirical studies of GIN in N Europe
- The model applies to *Ostertagia ostertagi*, and possibly to co-infecting *Cooperia*

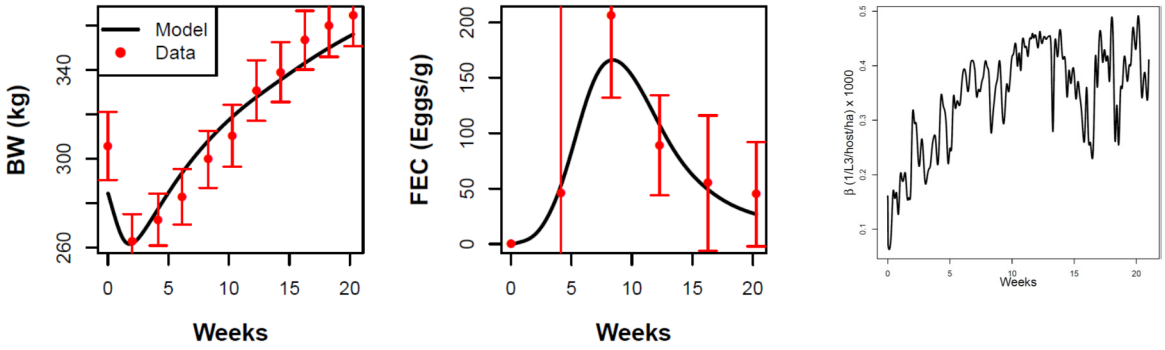

https://www.lmcni.com/

ABSTRACT

Gastrointestinal nematode (GIN) infections are ubiquitous and often cause morbidity and reduced performance in livestock. Emerging anthelmintic resistance and increasing change in climate patterns require evaluation of alternatives to traditional treatment and management practices. Mathematical models of parasite transmission between hosts and the environment have contributed towards the design of appropriate control strategies in ruminants, but have yet to account for relationships between climate, infection pressure, immunity, resources, and growth. Here, we develop a new epidemiological model of GIN transmission in a herd of grazing cattle, including host tolerance (body weight and feed intake), parasite burden and acquisition of immunity, together with weather-dependent development of parasite free-living stages, and the influence of grass availability on parasite transmission. Dynamic host, parasite and environmental factors drive a variable rate of transmission. Using literature sources, the model was parametrised for *Ostertagia ostertagi*, the prevailing pathogenic GIN in grazing cattle populations in temperate climates. Model outputs were validated on published empirical studies from first season grazing cattle in Northern Europe. These results show satisfactory qualitative and quantitative performance of the model; they also indicate the model may approximate the dynamics of grazing systems under co-infection by *O. ostertagi* and *Cooperia oncophora*, a second GIN species common in cattle. In addition, model behaviour was explored under illustrative anthelmintic treatment strategies, considering impacts on parasitological and performance variables. The model has potential for extension to explore altered infection dynamics as a result of management and climate change, and to optimise treatment strategies accordingly. As the first mechanistic model to combine parasitic and free-living stages of GIN with host feed-intake and growth, it is well suited to predict complex system responses under non-stationary conditions. We discuss the implications, limitations and extensions of the model, and its potential to assist in the development of sustainable parasite control strategies.

Key words: helminth; *Ostertagia ostertagi*; *Cooperia oncophora*; climate; parasite-induced anorexia; mathematical model

1. Introduction

Gastrointestinal nematode (GIN) infections have significant health, welfare and economic impacts in cattle and other grazing-livestock species, often through the occurrence of sub-clinical disease (Armour, 1980; Charlier et al., 2020b; Fox, 1993). The dominant GINs of cattle in temperate climates are *O. ostertagi* and *Cooperia oncophora*, which cause parasitic gastroenteritis primarily in first grazing season (FGS) cattle (Forbes, 2020; Michel, 1969). The use of anthelmintic treatments remains a first line practice to safeguard the health and growth performance of grazing livestock. However, the sustainability of this practice is threatened by the emergence of anthelmintic resistance in cattle worldwide (Kaplan and Vidyashankar, 2012; Rose Vineer et al., 2020a) requiring alternative parasite control strategies to limit further development of resistance. Further challenges emerge with the increasing pace of climate change, which may affect parasite development, grass availability and host growth; these challenges require further decisions on how to adapt the management practices of grazing livestock (Skuce et al., 2013; Vercruysse et al., 2018). Mathematical models are an important tool for evaluating and comparing alternative treatment and management strategies given the practical difficulties of doing so in experiments (Smith, 2011). Such models are useful, for example, for evaluating targeted selective treatments applied to individuals on the basis of parasitological or performance indicators (Charlier et al., 2014; Höglund et al., 2013); and where the benefits of preserving parasite refugia (Hodgkinson et al., 2019; van Wyk, 2001) are balanced against the risks of reduced health and performance in untreated animals. Achieving these goals requires the availability of models that include the full life cycle of the parasite, as well as the dynamics of immunity, grass availability and consumption, and animal growth.

Models of the full-cycle transmission of the most pathogenic GIN in cattle, *Ostertagia ostertagi*, have been developed and applied to field data (Grenfell et al., 1987a; Smith and Grenfell, 1994), but while these models have incorporated host and free-living (FL) parasite stages and host acquired immunity, they have not included host performance traits (Smith, 1997). However, weight gain and feed intake are important variables in the host-parasite interaction as well as having economic significance due to reduction in gain, especially in young parasitized cattle (Bell et al., 1988; Coop and Kyriazakis, 1999; Symons, 1985). In practice, body weight, as well as parasite eggs in host faeces, can be monitored during grazing to guide the applications of anthelmintic treatment; and affordable technology for routine individual weighing is becoming increasingly available (González-García et al., 2018). Weight and intake have important roles in system behaviour and models thereof, not only as output variables but also because they affect parasite epidemiology. First, the rate at which infective larvae are ingested (transmission rate) (Grenfell, 1988) is controlled by the rate of feed intake, of which weight is a main determinant (NRC, 1987); it is also controlled by the density of grass on pasture (Henriksen et al., 1976; Nansen et al., 1988). Second, intake is reduced through parasite-induced anorexia (Bell et al., 1988; Coop and Kyriazakis, 1999). Models that incorporate host performance during infection with *O. ostertagi* have been developed (Berk et al., 2016a), but have not yet been incorporated with a realistic and parameterised model of the parasite FL stages, which has been developed separately (Rose et al., 2015). The aim of our paper is to contribute to the above goals by integrating these system layers, whilst also aiming to focus on fewer host performance variables than the previous models, in the interests of transparent model behaviour and simpler parameterisation.

Here, building on elements from the above models, we propose a dynamic transmission model of the full parasite lifecycle, parameterised for *O. ostertagi* in cattle using parameter estimates from literature sources. The model incorporates 1) parasite load, acquired immunity, and weight and feed intake as host variables, 2) FL parasite stages influenced by local weather and climate, and 3) variable grass biomass. This model allows, for the first time, to investigate the consequences of control practices on both parasitological and performance variables, while taking into account of variability in

98 weather and seasonality in climate. We tested (validated) model predictions against field data from
99 several studies in Northern Europe; these studies took place during the FGS and under natural
100 infection and immunity progression. In addition, we explored the potential of the model to predict the
101 impacts of simplified anthelmintic treatments, leaving the effects of alternative anthelmintic
102 treatments for later consideration. We anticipate there is potential to parameterise the model for
103 other GIN species of grazing ruminants, and to explore behaviour under future climate change. We
104 hypothesise that interactions between growth, grass availability and intake, infection and immunity,
105 and the dynamics of the parasite pasture stages, lead to interpretable non-linear responses in system
106 behaviour, and that these can be explored to enhance the outcomes of treatment interventions.
107 Further, we hypothesise that when calibrated to conditions in published experimental trials in FSG
108 cattle, the model will reproduce observed patterns of animal infection and performance.

109

110 **2. Materials and Methods**

111 *2.1 Overview of the full transmission model*

112 The model of GIN transmission in a herd of grazing cattle, including the full lifecycle of the parasite,
113 links four sub-models schematised in Fig. 1. Two sub-models describe the animal host and its
114 interaction with the parasite. First, the host infection and immunity sub-model (Section 2.2) describes
115 host daily ingestion of infective third stage larvae (L3) on herbage, L_{3h}, from the current grass G on
116 pasture (determined by the daily grass intake, i.e. feed intake, FI, and its contamination L_{3h}/G), the
117 development of parasitic larval stages L (including L4 and L5) into adult worms W that produce eggs
118 excreted via the host faeces onto pasture, E_p, and the development of acquired immunity, I_m, by the
119 host concomitantly with its gradual infection. Second, the host growth sub-model (Section 2.3)
120 describes the bodyweight (BW), FI and growth of the host given its genetic propensity for growth, age,
121 current level of infection (since the start of grazing, or turnout onto pasture), and the current immune
122 state and response to the parasite loads L and W. The daily grass intake FI is calculated based on the

current BW and maintenance functions; the faecal mass output is the non-digested intake and is used to calculate the current number of parasite eggs excreted per unit mass (faecal egg counts) given the current number of eggs produced by the resident worms.

Two further sub-models describe the grazing environment and the survival of the FL parasite population. First, the grass growth model (Section 2.4) describes the availability of grass G through the grazing season in terms of dry mass per unit area of pasture, balancing grass growth and consumption through gazing by the herd; a net decrease in G will increase the larval concentration on herbage, L_{3h}, and its ingestion. Increases in intake during the host's growth trajectory, as well as parasite-induced anorexia will also affect L3 ingestion. Second, the FL-stages model (Section 2.5) describes the development of parasite stages outside the host, from eggs excreted in host faeces, through intermediate first and second larval stages, L_{12}, that reside within the faeces, and into infective larvae on pasture, which migrate in both directions between herbage, L_{3h}, and soil, L_{3s}, and while present on grass can be ingested through grazing. The development, survival and migration of these life stages depends on daily temperature and rainfall. The dynamics of the full transmission cycle are summarised by the parasite's effective reproduction number, R_e, which incorporates magnification or decline from each lifecycle stage through the effects of the weather and host-parasite interaction.

The full transmission model was built by linking the four sub-models and establishing suitable interactions between host, parasite and grass variables, and between the hosts in the herd who share the FL parasites and the available grass. For tractability, the implementation of the model is deterministic, i.e. each set of input conditions generates a single model prediction. For simplicity, the grazing host population (herd) is characterised by a stocking density per hectare, and the host sub-models are assumed to represent the average state of the animals in the herd; individual demographic stochasticity is not included. The grazing movement and the grass intake and L3 ingestion by the animals are represented in an average sense, assuming spatially-mixed grass consumption and faecal

148 deposition across the pasture; this is a mean-field rather than a spatially-explicit representation of the
149 host-environment interactions. Parasites in all stages are also treated at a population mean level.
150 These assumptions are shared by the past mathematical models of GINs in FGS cattle that we have
151 built on, which have similarly focused on *O. ostertagi* (Berk et al., 2016a; Grenfell et al., 1987a; Rose
152 et al., 2015). Each sub-model and supporting literature are described in detail next. All state variables
153 and parameters of the model are described in Tables 1-4.

154 *2.2 Sub-model 1: Host infection and immunity*

155 The model dynamics of host infection are as follows. The influx (J) of third stage infective larvae (L_3)
156 by a grazing animal at a given time (t) during the FGS is given by

$$J = FIDM\, L_{3c} = \beta\, L_{3p}\,, \qquad (1)$$

157 where FIDM is the animal's rate of dry matter intake and L_{3c} is the concentration of L3 on grass (as
158 distinct from the density of L3 per unit area, L_{3h}; Table 1). The second equality in Eq. (1) is for later use;
159 it involves the rate of transmission per infective larva (β) and the density of L3 on pasture (L_{3p}). In cases
160 where a dose of L3 is inoculated at turnout, as part of experimental trials used to validate the model,
161 there is an additional pulse in J at t=0. Ingested L3 that survive during establishment develop into stage
162 L (combined stages L4 and L5) before developing to dioecious adult worms. This development is
163 represented through n_L mathematical compartments, or phases (L_i, i=1…n_L), that confer a gamma
164 distribution to its time duration:

$$\frac{dL_1}{dt} = \varepsilon' J - \sigma L_1 \qquad (2)$$

$$\frac{dL_i}{dt} = \varepsilon' \sigma L_{i-1} - \sigma L_i \quad (i = 2, \ldots, n_L),$$

165 with $L = L_{nL}$ and ε' the probability of establishment (Table 1). This gamma distribution (in fact Erlang) is
166 used instead of the common exponential distribution (n_L=1) in order to ensure that pre-patency does

not end prematurely and has the expected duration (Leclerc et al., 2014). The choice n_L=5 ensures also that the distribution of times is approximately normal. Stages L become adult worms (W) at rate

$$\frac{dW}{dt} = \varepsilon' \sigma L - \mu W, \quad (3)$$

Eggs are produced by female adult worms at rate (Epd)

$$\frac{dE}{dt} = f_e(I_m, W)\, p_f\, W, \quad (4)$$

where f_e is the effective fecundity rate, which is reduced by the level of acquired immunity (I_m) and by the worm density

$$f_e(I_m, W) = f(I_m)\left(\frac{W_s}{W_s + W}\right)^{0.5}, \quad (5)$$

and where fecundity $f(I_m)$ is constrained by immunity but not by density. We modified the form of this density dependence in relation to (Berk et al., 2016a; Bishop and Stear, 1997) such that $f_e = f(I_m)$ when W is small.

The faecal egg count (FEC) is the egg output per gram of daily wet faecal output

$$FEC = \frac{Epd}{Faeces} = \frac{f_e(I_m, W)\, p_f\, W}{Faeces}, \quad (6)$$

where Faeces (Table 2) is the wet faecal output (calculated in Eq. 22) expressed as grams/d. FEC observations are usually based on faecal samples across the herd or pasture and thus represent an average over the grazing herd.

Three within-host parasite traits, L3 establishment, adult worm mortality, and female worm fecundity, are regulated by the host's immune response (Churcher et al., 2006; Grenfell et al., 1987b; Smith et al., 1987), each of which shifts between two parasite-specific limits as the level of immunity increases (Berk et al., 2016a):

$$\varepsilon(I_m) = \varepsilon_0 + (\varepsilon_1 - \varepsilon_0)\, I_m$$

$$\mu(I_m) = \mu_0 + (\mu_1 - \mu_0)\, I_m\,, \tag{7}$$

$$f(I_m) = \mu_0 + (\mu_1 - \mu_0)\, I_m^{nf}\,.$$

We assume that the first two responses develop at equal speed and that the reduction in worm fecundity occurs faster, via the exponent n_f <1 suggested by empirical observations (Dorny et al., 1997; Smith et al., 1987).

The level of acquired immunity is assumed to be bounded between 0 and 1; it is given by a sigmoidal growth function (here a von Bertalanffy-type function) of the cumulative exposure to L3 (C), given by

$$I_m(C) = \left(1 - (1 - I_m(0)) \exp\left(-\frac{C}{C_m}\right)\right)^3, \tag{8}$$

where $I_m(0)$ is the level of immunity at turnout, from when cumulative exposure is measured. In the FGS we expect $I_m(0)$=0.

The cumulative exposure C is a hypothetical memory of antigen stimulation from the incrementally ingested L3 (Smith and Grenfell, 1985); it emerges after a time delay required for the development of acquired effector mechanisms. The dynamics of C are represented in a similar way to the development of the within-host parasite stages,

$$\frac{dC_1}{dt} = J - \sigma_c C_1$$

$$\frac{dC_i}{dt} = \sigma_c\, C_{i-1} - \sigma_c\, C_i \quad (i = 2, \ldots, n_C - 1), \tag{9}$$

$$\frac{dC_{n_c}}{dt} = \sigma_c\, C_{n_c-1} - \mu_c C_{n_c}$$

with $C=C_{nc}$, and where we allow for loss of immunity through a constant-rate loss in C (μ_c). The equations for C are similar to those for L, but without mortality terms and with distinct rate parameters (Table 1). This representation builds on previous work (Anderson and May, 1985; Roberts and Grenfell,

1991; Smith and Grenfell, 1994) that related the theoretical level of acquired immunity directly to the cumulative number of L3 ingested and where immunity had a constant rate of loss. We expressed loss of immunity similarly, through a loss in the cumulative marker C; but rather than using C directly as immunity level, we used the bounded immunity level I_m (Eq. 8) for ease of interpretation because a given level of C is not directly interpretable (Rose Vineer et al., 2020b). A second difference in our representation is the distribution of the temporal delay in the emergence of C upon exposure; Eq. (9) prevents premature emergence by disallowing a skew towards zero. In addition, we assumed that the time scale of development of immunity is the same as that of the development of L_3 into adult worms (Table 1); this is a minimal working assumption as immunity could develop faster or more slowly than the with-host parasite stages; however, we have no evidence in favour of either case. A similar remark applies to the time delay; amid lack of evidence we assumed that the number of development compartments n_C is the same as n_L in the development of adult worms, which could be revised amid fresh evidence. Hypobiotic arrest and re-emergence of parasitic larvae, which is affected by season and immunity (Charlier et al., 2020a) was not included since this comes into play only towards the end of the grazing season, and is in any case too poorly understood to parameterise.

Table 1. Host infection and immunity. State variables and parameters defined in sub-model 1 (Section 2.2). State variables are time dependent. Parameters are constant or a function of the immunity level.

Variable	Description	Units	Comments
J	intake of L3 larvae	larvae/d	Eq. (1)
L_{3c}	L3 concentration on grass	larvae/kgDM	$L_{3c}=L_{3h}/(G/A_g)$ sub-model 3
L_{3h}	L3 density on herbage	larvae/ha	Sub-model 4
FIDM	Feed intake dry matter (DM)	kg DM/d	Sub-model 2
L_i	Development compartments between L3 and L	-	Number within host, i=1…n_L
L	Larvae stage pre-adult (fourth and fifth)	-	Number within host (L= L_{nL})
W	Adult worms in host	-	-
E	Cumulative number of eggs produced by adults	-	-
Epd	Eggs produced daily by female worms	eggs/d	-
FEC	Average faecal egg counts	eggs/g	per daily wet faeces (Eq. (6))
C	Marker of cumulative exposure to L3	-	Unbounded
I_m	Level of acquired immunity of the host	-	Bounded between 0 and 1
Parameter		**Units**	**Value**	**Source**
$\varepsilon(I_m)$	Establishment probability from L3 to adult	-	-	[1], Eq. (7)
ε'	Per-compartment establishment probability of L3	-	$\varepsilon' = \varepsilon^{\wedge}(1/n_L)$	-
ε_0	Establishment probability of L3 (naïve animal)	-	0.60	[2]
ε_1	Establishment probability of L3 (immune host)	-	0.05	[2]

σ	Development rate of L3	1/d	n_L/T_L	-
T_L	Mean pre-patency	d	32	[3]
n_L	Number of L_i development compartments	-	5	This paper
$\mu(I_m)$	Mortality rate of adult worms	1/d	-	Eq. (7)
μ_0	Mortality rate of adult worms (naïve host)	worms/d	0.025	[2, 4, 5]
μ_1	Mortality rate of adult worms (immune host)	larvae/d	0.06	[2, 6]
p_f	Proportion of female adult worms	-	0.55	[2]
$f_e(I_m,W)$	Effective fecundity rate of female adults worms	eggs/d	-	[7, 8]
W_s	Adult worm scale of density dependence	-	15000	[7, 9]
$f(I_m)$	Fecundity rate of worms (no density dependence	eggs/d	-	Eq. (7)
f_0	Fecundity rate of worms (naïve host)	eggs/d	350	[7, 10]
f_1	Fecundity rate of worms (immune host)	eggs/d	30	[7, 10]
n_f	Exponent relating f to I_m	-	0.2	This paper
$I_m(0)$	Initial level of immunity of host	-	0	FGS, or as stated
C_m	Cum. L3 exposure at ~25% of maximum immunity	-	70k	[2, 6]
σ_C	Development rate of C	1/d	n_C/T_C	-
T_C	Mean time of development of C	d	32	See T_L
n_C	Number of C development compartments	-	5	This paper
μ_C	Rate of loss of host immunity	1/d	ln(3)/180	[11]

[1] Includes mortality or arrest at rate (1-ε') σ. Rate of transition to the next compartment: ε' σ.

[2] Verschave et al. (2014)

[3] Assuming the observed 21d (Anderson, 2000; Verschave et al., 2014) corresponds to the 25th percentile of the gamma distributed development time assumed in Eq. (9) with shape parameter n_C.

[4] Michel et al. (1973)

[5] Grenfell et al. (1987b)

[6] Smith (1994)

[7] Berk et al. (2016a)

[8] Bishop and Stear (1997)

[9] Michel (1969)

[10] Smith et al. (1987)

[11] Mapped from an assumption of 70% decay in overall immunity level in 180d (Rose Vineer et al., 2020b).

2.3 Sub-model 2: Host growth

The variables and parameters of this sub-model are detailed in Table 2. The body weight (BW_n) of a naïve host (FGS calf that has not yet been infected) is assumed to increase with age according to a Gompertz function (Berk et al., 2016a; Forni et al., 2009),

$$BW_n = BW_m \exp\left(-\ln\left(\frac{BW_m}{BW_0}\right)\exp\left(-b\,(a - a_0)\right)\right), \quad (10)$$

where the growth rate (b) and mature weight (BW_m) are performance parameters inherent to the host species and breed, and BW_0 and a_0 are weight and age at turnout. The rate of weight gain is given by

$$\frac{dBW_n}{dt} = b\, BW_n \ln\left(\frac{BW_m}{BW_n}\right), \quad (11)$$

where t is time since turnout. The daily digestible (D) DM feed intake ($FIDDM_n$) is utilised by the animal as DM weight gain and in dry-mass flows associated with maintenance functions ($D_{maint,n}$):

$$FIDDM_n = p_{dry,n} \frac{dBW_n}{dt} + D_{maint,n} \quad (12)$$

where $p_{dry,n}$ is the proportion of gain that is DM, and $D_{maint,n}$ is expressed as DM.

An infected animal has reduced growth in relation to its potential growth if uninfected (Eq. (10)) because it has reduced intake (parasite-induced anorexia) and there are costs associated with infection (Coop and Kyriazakis, 1999; Coop et al., 1977; Fox et al., 1989). To derive the body weight (BW) and feed intake (FIDDM) of the infected animal we assume that, at a given time, its intake is suppressed by a factor A<1 in relation to that of the naïve (uninfected) animal of the same weight,

$$FIDDM = A\, FIDDM_n\,, \quad (13)$$

where 1-A is the proportion of reduction in FI caused by anorexia; it is also possible to have A>1 during compensatory growth. We assume, furthermore, that intake resources are used in additional mass flows (Coop and Kyriazakis, 1999) associated with functions that tackle infection ($D_{infection}$):

$$FIDDM = p_{dry} \frac{dBW}{dt} + D_{maint} + p_{dry}\, D_{infection}\,. \quad (14)$$

We expect the maintenance costs of the infected and naïve animals to be the same when they have the same BW. Rewriting Eq. 14 and substituting in Eqs. 11-13, we derive the rate of gain of the infected animal as being:

$$\frac{dBW}{dt} = A\left[b\, BW \ln\left(\frac{BW_m}{BW}\right) + \frac{D_{maint}}{p_{dry}}\right] - \frac{D_{maint}}{p_{dry}} - D_{infection}\,, \quad (15)$$

where A, D_{maint}, $D_{infection}$ and p_{dry} are specified below in terms of dynamic state variables of the animal. Some previous models of parasite burden include a simplified form of host growth for the purpose of

calculating faecal mass and egg output where BW is not related to infection state (e.g. Rose Vineer et al. (2020b); Singleton et al. (2011)), or with a different interaction between growth and parasite burden (Louie et al., 2007). We expect that in a non-infected animal A=1 and $D_{infection}$=0, giving the same gain as for the naïve animal (Eq (11)). In taking resources out of the allocation to growth in Eq. (15), a prioritisation in resource allocation to maintenance and infection functions (Doeschl-Wilson et al., 2008) is implicit.

The DM cost of maintenance can be expressed approximately in terms of metabolic weight, $BW^{0.75}$ (Archer et al., 1997) assuming near thermal neutrality (Supplementary Text S1):

$$D_{maint} = C_{maint} BW^{0.75}, \quad (16)$$

where C_{maint} is a parameter (Table 2). We assume that the costs of infection arise from the increment in the level of immunity (dIm/dt), the maintenance of the level of immunity I_m already acquired (Greer and Hamie, 2016), and the repair of damaged tissue associated with the current worm burden:

$$D_{infection} = C_{I1} \frac{dI_m}{dt} + C_{I2} I_m + C_W W, \quad (17)$$

where C_{I1}, C_{I2}, C_W are parameters (Table 2). Values of the parameters that are new, such as C_{maint}, C_{I1}, and C_{I2} are derived through relationships to other trait parameters reported in the literature (Supplementary Text S2). In this paper we focus on the immunity-related losses and neglect the cost (C_W=0) of repairing worm-induced damage to the intestine, which is thought to be comparatively smaller (Houdijk et al., 2001).

The DM proportion of gain, p_{dry}, is obtained by using an empirically-supported allometric relationship between body water content (Wt) and empty BW (eBW) (Carstens et al., 1991; Filipe et al., 2018), i.e. $W_t = a_w\ eBW^{bw}$, where a_w and b_w are allometric parameters, and which, upon differentiation gives

$$p_{dry} = \frac{d(BW - W_t)}{dBW} = 1 - b_w a_w (BW\ p_{empty})^{b_w} p_{empty}, \quad (18)$$

where p_{empty} is the proportion of BW that excludes gastrointestinal tract content (Williams et al., 1992).

The daily feed intake DM (FIDM) is obtained from the FIDDM (Eq. 12 or 13) by accounting for the apparent digestibility of grass DM (DDM) (Colucci et al., 1982):

$$\mathrm{FIDM} = \frac{\mathrm{FIDDM}}{\mathrm{DDM}}. \tag{19}$$

There is evidence DDM is not significantly affected by *O. ostertagi* and other GINs (Fox et al., 1989; Roseby, 1973; Taylor et al., 1989); here, it is assumed to be constant throughout the season (Table 2). Substituting Eq. 12 for FIDDM and Eqs. 14-15 for the remaining terms, Eq. 19 gives

$$\mathrm{FIDM} = \frac{\mathrm{A}\left(\mathrm{p_{dry}\ b\ BW\ ln}\left(\frac{\mathrm{BW_m}}{\mathrm{BW}}\right) + \mathrm{C_{maint}\ BW}^{0.75}\right)}{\mathrm{DDM}}, \tag{20}$$

where BW and p_{dry} are given by Eqs. 10 and 18, and the anorexia-related factor A is described below. Note that the term with brackets is the FIDDM of a naïve animal with the same BW. The actual intake was constrained by the capacity of the gastrointestinal tract, which was assumed to be approximately proportional to BW (Text S3).

The daily faecal output that is DM is the total DM intake, FIDM, subtracted of the digestible intake:

$$\mathrm{FaecesDM} = \mathrm{FIDM}\ (1 - \mathrm{DDM})\ . \tag{21}$$

The corresponding daily wet faecal output is:

$$\mathrm{Faeces} = \frac{\mathrm{FaecesDM}}{\mathrm{pFaecesDM}}. \tag{22}$$

where pFaecesDM is the proportion of faecal output that is DM. For simplicity, pFaecesDM is assumed to be constant at 0.15 throughout the season and across studies (Table 2), although its variability is a known source of uncertainty in FEC observations (Denwood et al., 2012; Le Jambre et al., 2007). The average host FEC (Eq. (6)) is calculated using this dynamically varying prediction of wet faecal output.

The parasite-induced reduction in FI is thought to be of the order of 20% to 30% (Bell et al., 1988; Coop et al., 1977; Sandberg et al., 2006); while its causes are not well established (Coop and Kyriazakis, 1999), it is believed to be related to the establishment of new adult worms (Coop et al., 1977), which in the case of *O. ostertagi* occurs in the abomasum (Fox, 1993), where maturation of L4 in the gastric gland provokes inflammation (Charlier et al., 2020a). Therefore, we assumed that A is driven largely by the rate of change in the number of adult worms (dW/dt):

$$A = \exp\left[q \tanh\left(\frac{dW}{dt}\frac{1}{DW_{max}}\right)(1 - I_m)^{0.3}\right]. \quad (23)$$

where q = ln(0.8) (Table 2) determines the lowest proportion to which feed intake can be reduced. The function tanh(x), which ranges from -1 to 1, and the scale parameter DW_{max} constrain the effect of dW/dt when its magnitude is of order DW_{max} or greater. When worm load increases (dW/dt>0, tanh(x)>0) then A<1 because q<1; and when the worm load decreases (dW/dt<0, tanh(x)<0) then A>1. Therefore, in the model it is possible to have compensatory growth briefly while the worm number is stabilising, e.g. after the onset of an immune response on worm mortality or after drug treatment. Empirical observations of rebound in BW or FI at a faster pace than may be expected at current BW (Bell et al., 1988; Coop et al., 1977, 1982; Fox et al., 1989; Szyszka et al., 2013) provide suggestive evidence that compensatory growth may occur under these conditions. Such rebounds in appetite and FI, observed rapidly after anthelmintic treatments, are mimicked in the model upon clearing of establishing and adult parasites (Section 2.7), after which parasite-induced anorexia halts, i.e. A=1 as the worm load becomes constant. The immunity-dependent factor in Eq. (23) aims to modulate the magnitude of either effect (A<1 or A>1) when immunity has developed; e.g. when anthelmintic treatment is applied and, following its effects, the worm burden rebounds but immunity has not been lost. The effect of A on FI during compensatory growth was constrained by the capacity of the gastrointestinal tract (Text S3). Other models have made different attempts at incorporating parasite-induced reductions in feed intake based on host variables related to L3 exposure (Berk et al., 2016a;

296 Grenfell, 1988) or adult worm burden W (Louie et al., 2007), while we assumed that change in appetite
297 is driven by change in W.

298 It has been reported that grazing cattle can have a short-lived drop in BW at the point of turnout
299 caused by a drop in FI and gastrointestinal content (Balch and Line, 1957; Fox et al., 1989) due to
300 adaptation to grazing. We represented this BW drop through a rapid reduction factor in feed intake
301 (Text S4). This correction to intake was applied when modelling empirical studies that exhibited this
302 additional behaviour and when exploring model behaviour.

303 **Table 2. Host growth.** State variables and parameters defined in sub-model 2 (Section 2.3). State
304 variables are time dependent or may depend explicitly on other variables, e.g. p_{dry}(BW).

Variable	Description	Units		Comments
BW	Body weight of an infected animal	kg		[1,2]
dBW/dt	Rate of BW gain per unit time	kg/d		[1]
t	Time (difference a- a_0 in age of animal) since turnout	d		Eq. (10)-(11), Supp. Text S2
FIDDM	Feed intake, digestible dry matter, of an infected animal	kgDM/d		[1, 3]
FIDM	Feed intake, dry matter, of an infected animal	kgDM/d		[2, 4]
FaecesDM	Faecal output, dry matter	kgDM/d		-
Faeces	Faecal output, wet	kg/d		FaecesDM/DDM
p_{dry}(BW)	Proportion of gain that is dry matter at current BW	-		[1]
Wt	Body water content (of the gut-empty body)	kg		a_w eBW^{bw}
eBW	Empty body weight, excludes gut content	kg		p_{empty} BW
D_{maint}	Rate of biomass used for maintenance functions	kgDM/d		[1, 3]
$D_{infection}$	Rate of biomass used for infection-related functions	kg/d		-
dIm/dt	Rate of increase in acquired immunity per unit time	1/d		-
A(Im,dW/dt)	Anorexia-induced change in FI in an infected animal	-		[4], <1 or >1
Parameter		**Units**	**Value**	**Source**
BW_m	Mature body weight of host	kg	variable	[5]
BW_0	Initial BW at age a_0	kg	variable	[5]
b	Rate of host growth or inverse time scale of growth	1/d	variable	[5]
C_{maint}	Rate of biomass used for maintenance functions	$kg^{0.25}$/d	0.03	[6], Supp. Text S1
C_{I1}	Rate of biomass used to increase the immunity level	kg/uI	10	[6], Supp. Text S2
C_{I2}	Rate of biomass used to maintain acquired immunity	kg/uI/d	0.4	[6], Supp. Text S2
C_W	Rate of biomass used to repair damage per adult worm	kg/d	0	This paper
p_{empty}	Proportion of BW that excludes gut content	-	0.91	[7]
a_w	Allometric magnitude of W in relation to eBW	-	1.997	[8]
b_w	Allometric exponent of W in relation to eBW	-	0.707	[8]
DDM	Apparent digestibility of DM grass	-	0.80	[9]
Exp(q)	Proportion of FI after reduction due to anorexia	-	0.80	[10]
DW_{max}	Scale controlling the nonlinear effect of dW/dt on A	worm/d	4000	This paper
pFaecesDM	Proportion of DM in faeces	-	0.15	[11]

[1] Variables with underscore n refers to the naïve (not-yet infected) animal.

[2] In some empirical studies BW dropped at turnout (Balch and Line, 1957), which was included through a temporary drop in FI (Text S4).

[3] DM: dry matter content. Other content is inclusive of water, if applicable.

[4] FI is limited by gastrointestinal tract (gut) capacity (Text S3).

[5] In the baseline model, literature values were used, BWm=700 kg, b=1/150d (Berk et al., 2016a; EBLEX, 2013). In model validation, involving differing cattle breeds, values were estimated from the group of non-infected animals.

[6] C_{maint} does not currently include the smaller contribution to maintenance costs associated with physical activity such as grazing. uI expresses units of immunity, up to a maximum of 1.

[7] Williams et al. (1992)

[8] Carstens et al. (1991)

[9] Bines et al. (2009); Colucci et al. (1982); Hart et al. (2009); Johnson et al. (2019)

[10] Bell et al. (1988); Sandberg et al. (2006)

[11] Moore (1978); Nennich et al. (2005); Smith et al. (1987)

305

306 *2.4 Sub-model 3: Grass growth*

307 The grass DM available for gazing (G) in a given area of pasture (A_g), is assumed to be controlled by:
308 the rate of grass growth per ha (r_g); a carrying capacity per ha (K_g) that limits grass growth according
309 to characteristics of the grazing system; and the rate of grass intake by the grazing herd at given
310 stocking density (N_h) and average daily intake per capita FIDM (Table 2). The net rate of grass growth
311 is assumed to have the following growth and consumption terms:

$$\frac{dG}{dt} = r_g A_g \left(1 - \frac{G}{K_g A_g}\right) - FIDM\, H\,. \qquad (24)$$

312 where $H=N_h A_g$ is the number of hosts in the grazing system. Parameter values are given in Table 3. In
313 this formulation, growth is limited by local resources, i.e. when G/A_g approaches K_g growth stops and
314 any further grazing will lead to decrease in sward availability, as is observed (Dimander et al., 2003;
315 Larsson et al., 2006). The assumed value of G at turnout (Table 3) is such that the grazing system has
316 not yet reached its limit capacity; hence, some increase in G ($dG/dt>0$) is possible upon moderate
317 consumption. Equation (24) assumes that the grass plants are only increasing in size and not
318 propagating in number; the opposite assumption can be made through logistic growth, where the
319 growth term in Eq. (24) would be multiplied by G (Grenfell, 1988; Louie et al., 2007). In using empirical
320 measurements of r_g (Table 3) we have assumed that these were obtained without, or were discounted
321 for the latter density effects, which is an approximation. Other authors have chosen not to include

such limiting effects in grass growth (Berk et al., 2016b). The rate of grass growth and the carrying capacity are currently assumed to be constant throughout the season. In addition, in the current non-spatial formulation, all variables are assumed to be uniform across the grazing area: the herd grazes an evenly-distributed herbage and each animal grazes identically. The grass availability G/A_g is used to convert the density of L3 per ha into the concentration of L3 per kg DM (Table 1), used to calculate the ingestion of L3 per animal.

Table 3. Grass growth. State variables and parameters defined in sub-model 3 (Section 2.4).

Variable	Description	Units		
G	Grass DM available for grazing at a given time	kgDM		
Parameters		Units	Value	Source
K_g	Carrying capacity density of the grazing system	kgDM/ha	3500	This paper
G_0/A_g	Grass DM density of the grazing system at turnout	kgDM/ha	2500	[1, 2, 3]
A_g	Area of pasture available for grazing	ha	1	-
r_g	Rate of grass growth per hectare	kgDM/ha/d	70	[1, 4]
N_h	Stocking density of grazing animals	-	5	[1, 2]
H	Number of hosts in the grazing system	-	N_h Ag	-

[1] UGS (2010)
[2] EBLEX (2013)
[3] Berk et al. (2016b)
[4] GrassCheck (2021)

2.5 Sub-model 4: Free-living stages

A model of the dynamics of the parasite's FL stages has been fully developed previously (Rose et al., 2015). Building on past work (Grenfell et al., 1987a; Smith, 1994), the GLOWORM-FL model incorporated the migration of infective L3 larvae between soil and herbage and the influence of weather variables on this movement. The model also contained fresh estimation of the influence of weather on the remaining parameters controlling the FL stages. In the current paper, we have added to this sub-model two dynamic flows linking the nematode FL and parasitic stages: the deposition of eggs in faeces and the ingestion of L3 by every host in the grazing herd. We briefly describe the model's variables and parameters (Table 4) and the additions to the model. Details, including parameter values for *O. ostertagi* are given in Text S4.

The dynamics of the FL living stages, including deposited eggs (E_p), stages developed within faecal pats (L_{12}, L_{3f}), and L3 on pasture (L_{3p}), on herbage L_{3h}, and on soil (L_{3s}), are defined as densities per ha and given by the rate equations (Rose et al., 2015):

$$\begin{aligned}
\frac{dE_p}{dt} &= E_{in} - (\mu_1 + \delta) E_p \\
\frac{dL_{12}}{dt} &= \delta E_p - (\mu_2 + \delta) L_{12} \\
\frac{dL_{3f}}{dt} &= \delta L_{12} - (\mu_3 + m_1) L_{3f} \\
\frac{dL_{3p}}{dt} &= m_1 L_{3f} - (\mu_4(1 - m_2) + \mu_5 m_2) L_{3p} - \beta H L_{3p} \\
L_{3h} &= m_2 L_{3p} \\
L_{3s} &= L_{3p} - L_{3h} \\
\frac{dE_c}{dt} &= E_{in} ,
\end{aligned} \qquad (24)$$

All variables and parameters are described in Table 4. The assumed initial values of the variables at turnout are given in Supplementary Table S2. The last equation in Eq. (24), for the cumulative number of eggs deposited (E_c), was introduced by us for later use. The remaining equations are as in Rose et al. (2015), but with three exceptions. First, we have replaced the rate δ for 2δ in Rose et al. (2015). Second, the rate of egg deposition on pasture by all hosts per day per ha was 100 and is now replaced with:

$$E_{in} = Epd\, H/A_g , \qquad (25)$$

where Epd, H and A_g are as in Tables 1 and 3. Third, there is an additional term in the rate of change of L_{3p} representing the daily ingestion of L3 by every grazing animal per ha. This term required defining a new time-varying parameter. The average daily probability of ingestion per L3 per host ($\beta(t)$), known

as rate of parasite transmission or instantaneous rate of infection, is the ratio of the L3 ingested per grazing host per day per ha (FIDM m_2 L_{3p}/G) to the L3 available on pasture per ha (L_{3p}):

$$\beta(t) = \frac{m_2 L_{3p} FIDM}{L_{3p} G} = m_2 \frac{FIDM}{G}, \quad (26)$$

where FIDM (Table 2, Eq. 20) is determined by the host's BW, parasite burden and level of immunity; G (Table 3, Eq. 23) is the current grass biomass available for grazing; and m_2 (Table 4, Eq. 24) is the current weather-dependent availability of L3 on herbage. The ingestion term, β H L_{3p}, in Eq. 24 is analogous to the transmission term in other models (Grenfell, 1988; Grenfell et al., 1987a; Kao et al., 2000; Louie et al., 2005; Roberts and Grenfell, 1991; Singleton et al., 2011; Smith and Grenfell, 1985); the difference being in how β is defined, which we do in terms of a host state variable, grass mass, and environmental drivers. Other work defined β conceptually similarly in terms of constant quantities (Singleton et al., 2011), through the ratio FIDM/G with FIDM determined by grass mass and reduced by larval exposure (Grenfell, 1988), or as a function of host age (Louie et al., 2005). Predictions of β are provided later. Note that Eq. 26 feeds into Eq. 1, which closes the loop of interdependency of model variables.

Table 4. Free-living stages. State variables and parameters defined in sub-model 4 (Section 2.5) by Rose et al. (2015). The dependency of the parameters on temperature and precipitation is given in Supplementary Table S1.

Variable	Description	Units	Comment
E_p	Density of eggs on pasture	eggs/ha	-
E_c	Cumulative eggs deposited on pasture	eggs/ha	-
L_{12}	Density of L1 and L2 larvae in faeces on pasture	larvae/ha	-
L_{3f}	Density of L3 in faeces on pasture	larvae/ha	-
L_{3p}	Density of L3 in pasture migrated from faeces	larvae /ha	herbage and soil
L_{3h}	Density of L3 on herbage on pasture	larvae /ha	As in Table 1
L_{3s}	Density of L3 in soil	larvae /ha	-
Parameters		Units	Weather dependent
$\beta(\tau)$	Probability of ingestion (transmission) per L3 per host	1/d	Yes, new variable
δ	Rate of development from egg to L3	eggs/d	Yes (Supp. Table S1)
μ_1	Rate of mortality of eggs on pasture	eggs/d	*idem*
μ_2	Rate of mortality of L1 and L2 larvae in faeces	larvae/d	*idem*
μ_3	Rate of mortality of L3 larvae in faeces	larvae/d	*idem*
μ_4	Rate of mortality of L3 larvae in soil	larvae/d	*idem*

μ_5	Rate of mortality of L3 larvae on herbage	larvae/d	*idem*
m_1	Rate of herbage-soil migration of L3	larvae/d	*idem*
m_2	Proportion of pasture L3 that are on herbage	-	*idem*

368

369 *2.6 Reproduction number*

370 To characterise the increase or decrease of the parasite population, and thus whether it is controlled,
371 we quantify the average extent to which each individual parasite replaces itself during its lifetime. For
372 macroparasites, the basic reproduction number (R_0) is defined as "the average number of (female)
373 offspring per adult (female) worm that survive to reproduction in the absence of density-dependent
374 constraints" (Anderson and May, 1992; Tompkins et al., 2001). Heuristic (Anderson and May, 1992)
375 and formal (Heesterbeek and Roberts, 1995) calculations of R_0 have been provided for simple models
376 of parasites with direct cycles; they quantify the parasite's maximum replacement rate when its
377 inherent reproduction and survival traits are expressed to the full extent, typically early in an outbreak.
378 Here, we focus on the overall dynamics of the parasite population towards stability by considering the
379 effective reproduction number (R_e), which includes the regulatory effects imposed by the host and the
380 environment on each parasite stage (Churcher et al., 2006). Given that it is not straightforward to
381 calculate R_e amid the complexities of the current model (Filipe et al., 2005), R_e can be expressed via
382 the following time-varying factors:

$$\begin{aligned} R_e = {} & (L_3 \text{multiplication in host}) \\ & \text{x (egg multiplication on pasture)} \\ & \text{x (probability an } L_3 \text{ is ingested by a host)}, \end{aligned} \tag{27}$$

383 Each of these factors can be expressed approximately and respectively as:

$$R_e = \left(\frac{E_c}{C}\right)\left(\frac{L_{3h}}{E_c}\right)\left(\frac{\beta H}{\beta H + \mu_4(1-m_2) + \mu_5 m_2}\right) \tag{28}$$

In the first factor, E and C are the cumulative numbers of eggs produced and L3 ingested by a host; in the second factor, L_{3h} and E_c are the cumulative numbers of L3 on herbage and eggs laid on pasture; and the third term is the average proportion of L3 on pasture ingested by hosts, given by the ratio of the rate of L3 ingestion per day per ha (β H, Eq. 26) to the rate of L3 departure from pasture through ingestion or mortality per day per ha (β H + μ_4 (1- m_2) + μ_5 m_2). This calculation is heuristic and approximate in its use of ratios of cumulative numbers of outgoing to incoming parasites per stage. The cumulative aspect tackles the fact that, under time varying conditions, changes in incoming and outgoing parasite stages are not synchronous; as it would be difficult to incorporate time lags explicitly, the calculation is approximated through the use of time averages. In a parasite population that stabilises, we would expect R_e to become close to 1, indicating no increase or decrease. However, full stabilisation through the regulatory factors that reduce R_e may take time to unfold on the scale of a single season. In addition, there is variation in environmental conditions due to seasonal climate, weather and management actions likely to cause fluctuations before and after stabilisation. Nonetheless, a R_e that declines over time to magnitudes around 1 would provide a health check on the mutual consistency of the parameters of the host and free-living sub-models.

2.7 Model behaviour

2.7.1 Numerical implementation

The model was solved numerically using Euler's method with a time step of 0.1 day. This step is small enough at the scale of all processes represented in the model and thus is likely to lead to solutions with satisfactory numerical accuracy. Using a step smaller than 0.1 led to no observable difference in the model output. In addition, this accuracy was assessed on simpler models with known analytical solution, giving an acceptable relative error of 0.37% with step 0.1 d, 3.6% with step 1d, and 28% with step 10d. The model was coded in the R language and the results were generated using the free software R, version 4.1.1 (R Core Team, 2021. R: A language and environment for statistical computing. R Foundation for Statistical Computing, Vienna, Austria). A code of the model is available (Filipe, 2022).

2.7.2 Baseline system

Predictions of the model, as defined in Sections 2.2-2.5 using parameter values from literature, were validated using the approach in Section 2.8. In addition, we explored how the model captures the effects of key factors on the epidemiology and control of *O. ostertagi*. For this purpose, we used baseline conditions defined by a representative location of temperate weather in Northern Europe and a typical year among its records of daily weather. We chose as location Large Park Hillsborough, BT26 6DR in Northern Ireland (coordinates 54°27'06.6''N, 6°04'30.7''W). Weather data (daily mean temperature and total precipitation) for this location were collected from the E-OBS gridded dataset (Cornes et al., 2018). We chose 2014 as a typical year among the last 10 years of weather data (2011-2020) as the daily pattern and annual average of the temperature in 2014 were closest to those of the daily records averaged over 10 years. As a representative grazing period we used 01/05 to 25/09 (21 weeks) in 2014. Weather data were used raw, without smoothing. The weather variables are plotted in Supplementary Fig. S1.

The baseline parasitology at turnout had an average concentration of *O. ostertagi* on herbage of 200 L3/kgDM (Berk et al., 2016b), and assumed that no other FL stage overwintered (Supplementary Table S2). We note that in the model this is the actual level of L3 on herbage, while in a real system an observation of L3 on herbage is likely to be an underestimation of its actual level; e.g. an assumed level of 200 could correspond to an observed level of 100 or less. The baseline FGS calves were assumed to be naïve (parasite free and with no acquired immunity), to have a body weight of 200 kg at turnout and growth parameters as in Table 2, which led to a BW trajectory in the range 200-400 kg over the 21-week grazing period. Daily FI was assumed to drop at turnout (Section 2.3 and Supplementary Text S4) as observed in some of the empirical studies used for validation and often observed more generally (Balch and Line, 1957). The cattle herd was assumed to have a stocking density of 5 animals/ha (Table 3).

2.7.3 Behaviour explored

Assuming the model structure and the parameters values described in Sections 2.2-2.5, the behaviour of the baseline system was explored in a range of scenarios where one model parameter was varied at a time:

1) Effect of the initial level of herbage contamination, i.e. concentration of L3 on herbage at turnout: L_{3c} = 100, 200, 500 L3/kgDM (Michel et al., 1970).
2) Effect of the herd stocking density: N_h=1, 5, 7 animals/ha, where 1-5 is the range found in the empirical studies used for model validation.
3) Effect of one anthelmintic treatment differing in the timing of application: T1 = 0, 4, 8 weeks after turnout.
4) Effect of two anthelmintic treatments with the first treatment applied at turnout (T1=0) but differing in the time of application of the second treatment: T2 = 3, 5, 7 weeks from turnout.

A simplified drug treatment was modelled, with 100% efficacy in clearing establishing and adult parasite stages during 21d and with no effect afterwards. The variation of some grass-growth parameters (Table 3) was also explored but found to have limited influence on model behaviour under the current values of the other parameters. These explorations were not included in the results but confirmed that our choice of values for these parameters was not determining.

2.8 Model validation

2.8.1 Datasets

In order to test the predictions of the model defined in Sections 2.2-2.5, the literature was searched for empirical studies satisfying the following criteria:

1) The study was on FGS beef or dairy cattle (aimed at testing the model on predominantly naïve animals).

2) Longitudinal data were provided on BW and FEC (the most common field observations) from turnout until the end of the experiment; where other parasitological variables predicted by the model were reported these were also compared with the model predictions.
3) Artificial dosing with L3 larvae was not used during the course of the study or was used only at the point of turnout (aimed at allowing infections to occur naturally after completion of the parasite's full cycle through the environment).
4) The experiment contained a group of untreated animals (aimed at testing the model in the absence of anthelmintic treatment, and to ensure that treatment applications in the model overlay a plausible host response).
5) The experiment contained an additional group of animals treated prior to and after the point of turnout (aimed at using the weight data of this group as proxy data for the weight of non-infected animals); for this purpose of characterising growth the animals should be genetically similar, i.e. from a single breed or cross of breeds.
6) The study location and calendar dates were provided so that weather data for the duration of the experiment could be obtained.
7) The study location was in Northern Europe.

We identified six studies based on these criteria (Table 5). Studies with natural infections only: 1) Larsson et al. (2007); Larsson et al. (2006), and 2) O'Shaughnessy et al. (2015). One study where the animals were inoculated with lower doses of L3 at turnout: Höglund et al. (2018), comprising 1) dairy cattle and 2) crossbred cattle from dairy and beef breeds. Studies where the animals were inoculated with higher doses of L3 at turnout: 1) Dimander et al. (2003) and 2) Höglund et al. (2013). All studies took place either in Ireland or in Sweden. Data were available from tables, text or figures in each article.

479 All studies reported mixed infections comprising predominantly *O. ostertagi* and *C. oncophora* (Table
480 5). The model, which was designed for a single-species *O. ostertagi* infection, was compared with
481 these data as we lacked single species data.

482 **Table 5. Six empirical studies used for model validation.** Summary of the information provided.

Study	Location	Year	Duration (d)	Av. BW at turnout (kg)	Av. L3 on pasture at turnout (1/kgDM)	Dose at turnout (L3)	Stock. dens. (1/ha)	Additional measures	Co-infection *O. ostertagi* (%) vs *C. oncophora*, serial observations
O'Shaughnessy et al. 2015	Ireland	2012	124	165	200 [1]	-	1.4	L3c (SGS)	L3: 73%, 23%, 50% (SGS)
Larsson et al. 2006; 2007	Sweden	2002	148	189	250 [2]	-	5	L3c (Y1, Y2), W (tracers 3w prior housing)	L3:<50% all season; W: 30%
Höglund et al. 2018, dairy	Sweden	2016	142	306	[3]	5000 [4]	2.25	-	L3: 47%, 80% (PCR)
Höglund et al. 2018, cross	Sweden	2016	142	332	[3]	5000 [4]	2.25	-	L3: 17%, 47% (PCR)
Höglund et al. 2013	Sweden	2008	154	238	[3]	40000 [4]	2.4	W (tracers Y2, Y3)	W: 24%, 27%
Dimander et al. 2003	Sweden	1999	150	200	300	10000 [4]	5	L3c (Y1, Y2); W (Y4 tracers)	L3: 20%, 75%

[1] Based on SGS.
[2] Average of first two observations.
[3] No data provided (c.f. note in Section 2.7.2).
[4] Doses comprised equal proportions of *O. ostertagi* and *C. oncophora*. FGS, SGS: first and second grazing season. Y1, Y2: Year 1, Year 2.

483

484 *2.8.2 Validation approach*

485 For each empirical study, we compared the model predictions with the longitudinal observations of
486 BW (or gain plus average start weight, as provided), and FEC. These data were reported as averages
487 over the animals in each treatment group and at each time point from turnout to the end of the
488 experiment. Where available, we also compared with model predictions any L3 observations
489 throughout the experiment, and worm counts in tracer animals from within the untreated group or
490 that grazed the same paddocks in subsequent seasons. There were no data on feed intake. Weather
491 data (daily mean temperature and daily total precipitation) for the spatial coordinates and calendar
492 dates reported in each study were collected from the same source as the baseline weather and used
493 raw, without smoothing. The weather variables are plotted in Supplementary Fig. S1.

494 The local daily weather, initial L3 contamination of herbage, any inoculation dose at turnout, cattle
495 stocking density, and cattle breed growth parameters were the only quantities adjusted to describe
496 the conditions of each empirical study. While many other parameters could have differed among
497 studies, all other model parameters were assumed to be the same across all studies, i.e. there was no
498 model fitting to data. In one study (O'Shaughnessy et al., 2015), the FEC at turnout was positive, hence
499 it was necessary to assume initial non-zero values for the number of adult worms and immunity level.

500 Where no measures of L3 on herbage at turnout were available (Table 1), an initial herbage
501 contamination was assumed based on studies in comparable regions (Michel et al., 1970) following a
502 similar reasoning as for the baseline system. Using the model's predicted mean trajectory of L3
503 concentration on herbage, we drew a sample from a negative binomial distribution (Smith and
504 Guerrero, 1993) with this mean and an aggregation parameter k=1.4 (Verschave et al., 2015); the
505 samples' lower quartile was contrasted with the data in an attempt to account for low efficacy in the
506 field recovery of L3 (Kloosterman, 1971; Paras et al., 2018). As the breed of the animals differed across
507 studies and their growth parameters were unknown, the average BW of the group of treated animals
508 was used as proxy for the BW of a naïve animal of the same breed, which unlike the infected animals
509 is not affected by anorexia and infection costs; these BW data were used to estimate the performance
510 parameters of the Gompertz BW gain of the infected animals (Eq. 11). This estimation was derived
511 using the nonlinear model regression function nls of the software R, version 4.1.1 (R Core Team, 2021.
512 R: A language and environment for statistical computing. R Foundation for Statistical Computing,
513 Vienna, Austria). Standard errors for BW and FEC mean observations were provided in a minority of
514 studies and included in the plots where the model output and empirical data were compared.

515 To be able to tackle data from two-species co-infections (Section 2.8.1 and Table 5) and which do not
516 specify parasite numbers by species (except for occasional relative proportions in some studies), we
517 input the initial total concentration of L3 on herbage into the model and predicted the numbers of
518 parasitic and FL nematode stages as totals for both species, which we then compared with the data.

519 The working hypotheses are that: 1) the parameters and processes in the model are adequate for
520 describing each species and thus the total infection, and 2) there are no interactions between species.
521 In this way, the model is regarded as representing a typical parasite mixture with variable relative
522 proportions of *C. oncophora* and *O. ostertagi*. Alternatively, if we knew the proportions of observed
523 FEC and initial L3 corresponding to *O. ostertagi*, we could have modelled a single *O. ostertagi* infection
524 (Smith and Guerrero, 1993), which would nevertheless still assume no interactions between species
525 in the real system. Unfortunately, these proportions vary throughout the season (Högberg et al., 2021)
526 and are largely unknown as indicated by the rare measurements in the current studies (Table 5); this
527 was the case whether the animals were inoculated with known species mixtures at turnout or subject
528 solely to natural infection. For these reasons, we considered inevitable to take the above approach,
529 which is simple and easily interpretable.

530 *2.8.3 Statistical approach*

531 A statistical comparison between the BW and FEC predicted by the epidemiological model and the
532 empirical data was made using a standard validation approach (Mayer and Butler, 1993). In this
533 approach, the observed data are linearly regressed on the model output, i.e. the first is treated as a
534 response and the latter as a predictor; the intercept of the relationship is fixed at zero. The outcomes
535 of this regression are an estimated slope, a p-value on an F statistic assessing the fitted line against a
536 constant response, a 95% confidence interval (CI) on the estimated slope, and a coefficient of
537 determination adjusted for the number of model parameters (R^2_{adj}). If the p-value is significant, we
538 can reject the null hypothesis that there is no relationship between the observations and the model
539 (i.e. that there is no change in the observations the predictions change); we used the conventional 5%
540 significance level, but expect that only much smaller p-values would comfortably reject the null
541 hypothesis. If the 95% CI of the estimated slope includes the value 1, in addition to excluding the value
542 0, then there is statistical support for the epidemiological model as this indicates the overall deviation
543 between model and data is within the variation expected to occur within the data. An R^2_{adj} close to 1

544 supports the assumed linear relationship between the epidemiological model and the data. We report
545 the p-value, CI on the slope, and R^2_{adj}. The statistical analyses were done using the linear model
546 regression function lm of the software R, version 4.1.1 (R Core Team, 2021. R: A language and
547 environment for statistical computing. R Foundation for Statistical Computing, Vienna, Austria).

548

549 **3. Results**

550 *3.1 Model behaviour*

551 The response of the model to differing conditions was explored using the model structure and
552 parameters of Sections 2.2-2.5. Further results, on the validation of the model, are presented in
553 Section 3.2.

554 *3.1.1 Effect of the initial level of herbage contamination*

555 Varying the herbage contamination at turnout (L_{3c} = 100, 200, 500 L3/kgDM) caused a considerable
556 peak shift (earlier peak) in calf FEC and in adult worm burden (Fig. 2). A higher starting pasture
557 contamination caused an earlier, higher peak and an earlier decline in FEC. For the adult worm burden,
558 however, a higher initial contamination caused an earlier but lower peak and a later decline; this
559 difference can be due to the fact FEC is affected by additional and earlier effects, i.e. reduction in
560 fecundity due to acquired immunity and density dependence. The effects on BW were appreciable,
561 with greater differences in cumulative gain between 10-15 weeks, but were followed by some
562 recovery in lost gain and more modest BW differences by the end of season. The differences in
563 contamination at turnout were reflected in the temporal trajectories of L3 contamination, but were
564 much reduced by the end of the season.

565 *3.1.2 Effect of the herd stocking density*

566 Higher stocking densities (N_h=1, 5, 7 ha^{-1}) enhanced transmission and amplified infection pressure,
567 leading to earlier, higher peaks in worm burden and FEC, which then declined towards the end of the

grazing season (Fig. 3). At lower stocking densities, egg shedding from animals persisted longer due to lower levels of immunity. However as stocking density increased, pasture contamination increased markedly and persistently, as a result of a larger number of hosts shedding eggs and infective larvae developing from earlier, higher shedding. In addition, the greater parasite challenge at high stocking densities resulted in slower weight gain that produced persistent differences in body weight through to the end of the grazing period (Fig. 3). Across weather in different years, these patterns were robust but the strength of peak shifts in FEC and differences in BW by the end of season vary across years (not shown); e.g. these effects were stronger in 2011 than in the current example of 2014. Compared with increases in the initial pasture larval contamination, increases in stocking density drove later but more persistent differences in FEC, herbage larval level, and weight gain; and, for worm burden and FEC, differences mostly in magnitude rather than timing. These differences result from the time lag between host infection, through egg shedding to larval maturation, and from the greater number of hosts carrying and transmitting parasites. Note that the red curves are identical between Figs. 2 and 3. Increased L3 abundance late in the season at higher stocking densities (Fig. 3) could affect starting L3 levels in the next season (Fig. 2).

3.1.3 Effect of one anthelmintic treatment differing in the timing of application

A key management parameter when a single round of drug treatment is applied after turnout, is the timing of application during the grazing season. The model predicted that an intermediate time after turnout (among 0, 4 or 8 weeks post turnout) is optimal (Fig. 4) in the following sense: it led to greater cumulative BW gain and to lower cumulative parasite burden in the host, and thus to potentially lower risk of production loss and clinical disease, while still leading to end-of-season pasture contamination and parasite burden comparable to those of the late treatment. Early treatment (at turnout) delayed infection but also immunity, leading to higher overall worm burdens and late-season L3 levels than for the later treatments, although still lower than in the absence of any treatment (Fig. 3, red line).

3.1.4 Effect of two anthelmintic treatments differing in the timing of the second treatment

When two anthelmintic drug treatments are applied, it is natural to apply the first at turnout and to examine the best timing for application of the second treatment. The model predicted that when varying the latter (among 3, 5, 7 weeks post turnout), there was not much difference in the final BW (Fig. 5). In all cases, the lowered infection pressure led to lower levels of immunity, which allowed adult worm populations to continue increasing throughout the grazing period. However, there was considerable difference in the level of pasture contamination potentially carried over to the next season and in the cumulative parasite burden (Fig. 5), with the latest application being the best in this respect, but with the intermediate timing being next best.

3.1.5 Effective reproduction number

In the four model behaviour examples, the predicted effective reproduction number R_e exhibited a clear pattern (shown on a logarithmic scale, Fig. 2-5). In the initial phase R_e had very large values likely influenced by the assumed initial numbers of parasite stages and by specifics of the calculation of R_e (Eq. (28)). Hence, during this phase, we seek for meaning in pattern rather than in values. Subsequently, there was a sharp decline in R_e followed by oscillations within the range 10-1, i.e. above but not far from the value 1. This pattern confirms our expectations about the model output (Section 2.6): it indicates convergence to a state of quasi stability in the parasite population superimposed by short-term fluctuations, likely due to variation in host response and weather (the same in the four examples). In these examples, the curve with lowest final value of R_e does not always correspond to the case with the lowest final value of L3; we expect this to be because R_e is also affected strongly by parasite burden and the current level of feed intake.

3.2 Model validation

Predictions of the model defined in Sections 2.2-2.5 were tested against data from empirical studies. The studies were organised in pairs that had, respectively, natural infection (Fig. 6), a low artificial parasite dose followed by natural infection (Fig. 7), and a higher artificial parasite dose followed by natural infection (Fig. 8). These figures show the predicted BW, daily FI, FEC, and number of adult

618 worms per FGS calf, and the predicted L3 herbage contamination and R_e. The figures also show the
619 observations on BW and FEC and, where data were available, on other traits.

620 *3.2.1 BW and FEC*

621 Visual comparison of the predictions with the empirical data indicates the model was generally in
622 reasonable agreement with the BW and FEC data across the studies (Fig. 6-8). There is formal statistical
623 support for this agreement in almost all cases (Table 6): the 95% CI of the slope of the relationship
624 between observed data and prediction includes the value 1 and not the value 0 (as confirmed by a low
625 p-value) and the data relate linearly to the predictions (as indicated by a R^2_{adj} close to 1). Where SEs
626 were reported for BW and FEC (Höglund et al., 2018; O'Shaughnessy et al., 2015) and BW (Dimander
627 et al., 2003), the deviations between data and prediction were generally in reasonable agreement
628 with the estimated SEs (Fig. 6-8) except for the FEC in O'Shaughnessy et al. (2015); it is possible that
629 the latter SEs are conservative indicators of uncertainty as they have constant value and may not fully
630 account for overdispersion in egg counts. There was an exception, however, in the studies where the
631 animals were inoculated with larger L3 doses (Dimander et al., 2003; Höglund et al., 2013); here, the
632 magnitude of the peak of the FEC (at 5 weeks post turnout) was considerably underestimated by the
633 model (Fig. 8), although there was agreement at the remaining time points; possible causes are
634 discussed later.

635 **Table 6**. **Statistical tests on the relatioship between the datasets and the model predictions.** CI 95%:
636 confidence interval of the slope of the linear relationship between observation data and prediction.

Trait	Statistic	O'Shaughnessy et al. 2015	Larsson et al. 2006	Höglund et al. 2018, dairy	Höglund et al. 2018, cross	Höglund et al. 2013	Dimander et al. 2003
BW	p-value	6.76E-10	4.10E-12	1.23E-16	9.32E-18	7.71E-21	2.36E-09
BW	R^2_{adj}	0.99849	0.99909	0.99904	0.99943	0.99969	0.99935
BW	lower CI	0.993	0.981	0.987	0.983	0.997	0.918
BW	upper CI	1.067	1.031	1.029	1.015	1.019	0.969
FEC	p-value	0.00071	0.00010	5.92E-05	0.00356	0.01029	0.07687
FEC	R^2_{adj}	0.84926	0.77949	0.96251	0.81074	0.64229	0.39640
FEC	lower CI	0.474	0.458	0.882	0.733	0.758	-0.204
FEC	upper CI	1.067	1.17	1.341	2.184	3.757	2.815

637

3.2.2 L3 on herbage

The predicted L3 concentration on herbage was in less quantitative agreement with the data (Fig. 6 and 8) (Dimander et al., 2003; Larsson et al., 2006; O'Shaughnessy et al., 2015) than the predicted BW and FEC. In two out of three cases where data were available, the model overestimated the magnitude of the observations considerably, although in all cases the predicted time trend seems consistent with that of the data. There are, however, many factors, some of which method-related, that can limit the efficacy and cause variability in the field recovery of L3 (Cain et al., 2021; Kloosterman, 1971; Paras et al., 2018; Tontini et al., 2019; Verschave et al., 2015). In particular, the fact one or two of the L3 counts suddenly dropped to zero and then rebounded during the season (Fig. 6) could result from sampling variation, although some of these sample points occurred when L3 availability was predicted by the model to have dropped suddenly and temporarily due to climatic factors. In O'Shaughnessy et al. (2015) (Fig. 6), the reported L3 refer to the SGS and not to the current season; in Dimander et al. (2003) (Fig. 8), L3 are reported for both the current and the following grazing seasons.

3.2.3 Adult worms

The predictions of W were generally in reasonable agreement with the few data points from tracer animals (Fig. 6-8). In some cases (Table 5), these tracer animals grazed the same fields in a later grazing season, in which case the data may bear a weaker association to the original level of herbage contamination.

3.2.4 Effective reproduction number

The patterns in R_e are more variable across the empirical studies than across the model behaviour examples due to the greater variation across studies, which includes differing weather, host growth and parasitological conditions. Yet, these patterns are similar among each other and to those in the behaviour examples, albeit being more variable in the extent and range of the oscillations above, near and occasionally below 1. Overall, the more or less precipitous drop in R_e through the grazing season

662 is consistent with the challenge-dependent acquisition of immunity dampening the potential parasite
663 population growth.

664

665 **4. Discussion**

666 We developed a novel mathematical model of the epidemiology of GIN infections in gazing animals.
667 The model integrates variables describing the parasitic and FL stages of the nematode and the
668 performance (growth, feed intake) and immunological states of the host. The model further includes
669 compensatory host growth upon reduction in parasite load, the influence of weather on the parasite's
670 FL stage dynamics, and the influence of variable grass biomass on the ingestion of infectious parasite
671 stages by the host. While the parasite population model uses a well-established framework for the
672 dynamics of macroparasite infections (Anderson and May, 1978; Anderson and May, 1992) and
673 follows previous attempts for GINs in cattle (Grenfell et al., 1987a; Roberts and Grenfell, 1991; Smith
674 and Grenfell, 1994), the interactions with grass, weather data, and animal growth are novel and allow
675 for the exploration of climate-driven effects and eventually the optimisation of treatment strategies
676 based on performance as well as parasitological criteria. Therefore, we consider the inclusion of these
677 variables central to the use and further development of models as tools to help address the challenges
678 set out in the Introduction, i.e. the evaluation of alternative treatment and management strategies to
679 current practices required by emerging anthelminthic resistance and climate change. Our first
680 hypothesis, that the interactions within the model lead to interpretable nonlinear responses in the
681 system that can be explored to enhance the outcomes of parasite control interventions, was
682 supported by the study of model behaviour. Our second hypothesis, that the model is able to
683 represent patterns of animal infection and performance in experimental trials, was supported by the
684 outcomes of the model validation.

685 *4.1 Modelling approach and scope*

686 The model was parameterised, using literature sources, specifically for *O. ostertagi* in grazing cattle
687 in temperate climates. We did so because of the clinical and economic importance of this species,
688 particularly in young cattle (Armour, 1980; Charlier et al., 2020b; Forbes, 2020) and because of the
689 greater knowledge of the relevant parameters for this species (Grenfell et al., 1987b; Michel, 1969;
690 Michel et al., 1973; Rose et al., 2015; Smith et al., 1987; Verschave et al., 2014). In addition, model
691 predictions were tested (see below) against datasets on FGS as this comprises all young cattle and in
692 an attempt to develop and test the processes of acquisition of immunity from a known, naïve state,
693 which avoids confounding effects from parasitological history.

694 We integrated, for the first time, processes relating to infection and immunity in cattle with the
695 dynamics of the FL stages, grass availability and animal growth. Epidemiological models of the *O.*
696 *ostertagi* lifecycle have been previously developed (for reviews of models of GINs in cattle see (Cornell,
697 2005; Smith and Grenfell, 1994; Verschave et al., 2016a)), but stopped short of incorporating all these
698 factors. The first innovation added here is a model of the dynamics of parasite FL stages (Rose et al.,
699 2015) that extended earlier work (Grenfell et al., 1986, 1987a; Smith, 1990; Smith et al., 1986) by
700 including the influence of weather on soil-herbage migration, and to which we added egg shedding
701 and larva ingestion by the cattle herd (sub-model 4). The second innovation is a model of the dynamics
702 of the host state that builds on and adapts past work on parasite load and acquired immunity
703 processes (Grenfell et al., 1987a, b; Roberts and Grenfell, 1991; Smith and Grenfell, 1994) (sub-model
704 1) and adds further variables describing host growth similarly to Vagenas et al. (2007) and Berk et al.
705 (2016a); Berk et al. (2016b) (sub-model 2). Our host-state model differs from that of Berk in using
706 fewer host state variables, distinct parameters and parameter values, and a revised representation of
707 parasite-induced anorexia (Coop and Kyriazakis, 1999) on feed intake and the addition of
708 compensatory growth. We note also that Berk's model included a deliberately simplified
709 representation of the parasite FL stages, whose availability varied seasonally but not according to egg
710 output that developed under the influence of weather. Thirdly, our model includes (sub-model 3)

711 dynamic variation in grass availability (Grenfell, 1988), which influences both animal growth and the
712 concentration and hence the ingestion of parasite infective stages.

713 One novel aspect that emerged in this integrated model, is an explicit relationship of the rate of
714 parasite transmission, or instantaneous rate of infection, Eq. (27), to variables relating to the host,
715 parasite and grazing environment:

$$\beta = \frac{[\text{proportion of pasture L3 on herbage}] \text{ x } [\text{feed intake by a host}]}{[\text{grass biomass}]}. \qquad (29)$$

716 In Eq. (29), the proportion of L3 on herbage depends on the current weather; the feed intake depends
717 on the current host body weight and parasite burden; and the grass biomass concentration depends
718 on the grazing history and carrying capacity of the grazing system. Equation (29) builds on and adds
719 to previous work (Anderson and May, 1978; Grenfell, 1988; Grenfell et al., 1987a; Kao et al., 2000;
720 Louie et al., 2005; Singleton et al., 2011; Smith and Grenfell, 1985) a dynamic trade-off between host
721 and environmental variables. Models are often very sensitive to the value of β when β is treated as a
722 constant parameter (Grenfell et al., 1987a); in our model, however, β is a variable controlled by
723 simultaneously-changing variables whose effects may either add or counterbalance. Based on the
724 current parameters of the model, the variation of β during the grazing season was in the range 10^{-3} -
725 10^{-4}/day/larva/host (c.f. model behaviour example in Supplementary Fig. S2), in agreement with
726 estimates of β for *O. ostertagi* in cattle (Smith and Grenfell, 1985) and for other GINs in sheep (Kao et
727 al., 2000).

728 As the processes modelled are not specific to *O. ostertagi* (including not being specific to its abomasal
729 location, except possibly Eq. (23) the model has the potential to be re-parameterised for application
730 to other parasites with a similar direct lifecycle, i.e. where transmission occurs through free-living eggs
731 and larvae (Anderson and May, 1992; Smith and Grenfell, 1994). Such parasites include GINs in cattle
732 such as *Cooperia* species. First steps have already been taken in extending the FL-stage dynamics

(Grenfell et al., 1986; Sauermann and Leathwick, 2018) and the parasitic-stage dynamics (Rose Vineer et al., 2020b) to these species, although not yet in an integrated full-cycle model.

In principle, the model can also be adapted to GINs in other ruminant species. In fact, several full-cycle models have been developed for other ruminants (Verschave et al., 2016a) such as sheep (Kao et al., 2000; Louie et al., 2007; Singleton et al., 2011), incorporating similar essential mechanistic understanding and specific parameter estimates. Some of these models are simpler to analyse, parameterise and apply than the current model; however, most incorporate fewer state variables than would be necessary to describe host growth and immunity and the influence of weather and climate on parasite dynamics. The current model therefore offers advantages that might be extended to other systems, especially when seeking to predict outcomes and optimise interventions for both performance and parasite control, as recommended to attenuate the development of anthelmintic resistance (Charlier et al., 2014).

Given the many sources of uncertainty in the parasite and host dynamics, including uncertainty in the model parameters, reliable forecasting for a specific situation cannot be reasonably expected (Cornell, 2005; Grenfell et al., 1987a; Smith and Grenfell, 1994); this is even more so as strong influencers like weather and pasture contamination cannot be predicted at a future time. Instead, this and related models (Verschave et al., 2016a) are suited for predicting system responses to given parasite control strategies in order to classify their relative efficacies (Cornell, 2005; Smith, 2011). Therefore, agreement with observed patterns of infection and growth in published trials is important to build confidence in the use of the model under different conditions.

4.2 Model validation

We have demonstrated the ability of this new model to capture parasite and host dynamics in real systems through a validation exercise. Validation was carried out on empirical studies in Northern Europe reporting BW and FEC variables and containing a non-treated group. In addition, the animals in these studies were infected naturally through grazing such that the parasite dynamics were

758 controlled by weather and host-parasite interactions alone. Some studies included inoculation of L3
759 at turnout, but subsequent infection was exclusively through grazing. The model predictions
760 compared satisfactorily against the observations of BW and FEC across all studies, both graphically
761 and in formal statistical testing. However, there were two studies, whose animals were inoculated
762 with larger L3 doses at turnout, where the model underestimated considerably the magnitude of the
763 FEC peak, although there was good agreement at the remaining time points. One explanation for this
764 outcome stems from the fact that the animals were subjected to co-infection, predominantly by *O.*
765 *ostertagi* and *C. oncophora* (Table 5), as is typical in natural field infections (Henriksen et al., 1976;
766 Högberg et al., 2021; Michel et al., 1970), and that the FEC data used did not differentiate parasite
767 species. As *C. oncophora* has considerably higher maximum fecundity (prior to being regulated)
768 (Kloosterman et al., 1984; Verschave et al., 2016a; Verschave et al., 2014), a model parameterised for
769 *O. ostertagi* would be expected to lead to lower FEC prediction, particularly in studies where parasite
770 inoculated doses and loads are higher and at the peak of egg production, i.e. prior to the strong
771 regulation of fecundity imposed by the developing acquired immunity and worm burden. A similar
772 occurrence has been reported in previous model validation exercises (Smith and Guerrero, 1993).
773 Likewise, experimental studies have suggested that FEC may differ between species at its peak but not
774 necessarily at other time points (Hilderson et al., 1995; Kloosterman et al., 1984).

775 The use of studies with co-infection was imposed by a lack of data on single-species infections under
776 natural weather conditions, which is required in order to test a full-cycle model. However, testing
777 models under realistic field conditions, where co-infection by parasite species is common, can be
778 regarded as desirable. Nevertheless, given that the model was designed and parameterised for a single
779 parasite species, we, like others (Smith and Guerrero, 1993), are cautiously optimistic about the extent
780 to which the model can represent co-infection situations. As we described earlier, the initial L3
781 concentrations input in the model and the parasite loads predicted were interpreted as representing
782 total infection by both parasite species. Our working hypotheses were that: 1) there are no
783 interactions between the species within the host, and, 2) the parameters and processes in the model

784 are adequate for describing the dynamics of both species. Under these hypotheses, the model can be
785 regarded as representing a typical parasite mixture, where e.g. *C. oncophora* dominates early and *O.*
786 *ostertagi* dominates later (Dimander et al., 2003; Högberg et al., 2021). Regarding the first hypothesis,
787 there is no experimental evidence of interaction between the host responses to *O. ostertagi* and *C.*
788 *oncophora* in grazing calves (Dorny et al., 1997; Hilderson et al., 1995; Satrija and Nansen, 1993),
789 although there is some evidence of cross-immunity (Kloosterman et al., 1984). There is evidence of
790 interaction between co-infecting GINs of other species in cattle (Herlich, 1965) and in sheep and goats
791 (Basripuzi et al., 2020; Lello et al., 2018; Sykes et al., 2009). Accounting for possible interaction
792 between *O. ostertagi* and *C. oncophora* in cattle would require more experimental knowledge and
793 further model advancement (see below).

794 Regarding the second hypothesis of adequacy of our model to describe both parasite species, it is
795 likely that the same basic mechanisms are suitable to describe both species, at least at the level of
796 simplification of the models, e.g. the location of establishment in the gastrointestinal tract, which
797 differs between *O. ostertagi* and *C. oncophora*, is not specified in the model. However, there may be
798 differences in parameter values between parasite species, e.g. in rate of acquisition of immunity
799 (Dorny et al., 1997; Hilderson et al., 1995), although only some of the model parameters have been
800 quantified for both species (Rose et al., 2015; Rose Vineer et al., 2020b; Verschave et al., 2016a;
801 Verschave et al., 2014). One reason why the model may have approximated satisfactorily many of the
802 variables in these studies, is that several of the parameters may be similar enough between the two
803 parasite species (Grenfell et al., 1986; Rose Vineer et al., 2020b; Verschave et al., 2016b; Verschave et
804 al., 2014), and some of those that differ more could have contrasting effects on the overall dynamics,
805 e.g. through characteristics of the immune response vs fecundity, as suggested by experiments
806 (Hilderson et al., 1995). Moreover, where there are differences, we expect them to be greater when
807 egg production and parasite loads are higher, which, due to the regulatory effects of immunity and
808 density-dependency, may be relatively short-lived and occur predominantly near the peak of FEC.
809 Therefore, there is a cautious indication the model may, to a degree, be able to capture typical

seasonally-varying mixtures of these parasites in the field, although this is an area where future research is clearly needed.

Compared to the predictions of BW and FEC, prediction of the L3 concentration on herbage was in less quantitative agreement with the data (where available); the model overestimated the abundance of L3 on pasture relative to that observed, although the patterns of the predicted time trends were consistent with those of the data. However, many factors can contribute to low efficiency and sampling variation in the field recovery of L3. These factors include the recovery method and the analyst (Cain et al., 2021; Kloosterman, 1971; Paras et al., 2018; Verschave et al., 2015), differing grass growth and under-sampling of the sward at the lowest level (Tontini et al., 2019), soil-herbage migration of L3, and avoidance of faecal pats or dung beetles, which associate with higher L3 concentration (Henriksen et al., 1976; Nansen et al., 1988). Measurement variation within a study can result from limited sampling of highly aggregated L3, and this possibility cannot be excluded in the studies where L3 counts dropped to zero and rebounded during the season. On the other hand, the use of differing recovery methods can lead to differences in recovery rate between studies (Verschave et al., 2015). Therefore, we would not regard the above overestimation as significant. The predictions of worm counts, W, were generally in agreement with the small number of post-mortem counts from tracer animals, some of which grazed the same fields concurrently while others did so in subsequent years.

A very small subset of model parameters or variables was informed by factors reported in the studies used for validation. Factors that were not measured in these experiments may have influenced the observations. These could include weather (beyond temperature and rainfall, which were included in the model); management; initial pasture contamination; immune status (naïve); faecal moisture content; sampling variation of the FEC method used; density and growth of the grass biomass; apparent digestibility of grass DM and use of feed supplements; and genetic strength and speed of the immune response. As we did not have information on any of these factors and we were not fitting

835 the model to the data, we assumed that all remaining parameters of the model did not differ between
836 studies. Given the potentially unaccounted-for variables, the ability of the model to produce estimates
837 of parasite population and animal growth so close to observed values provides confidence in its ability
838 to predict system dynamics under different, broader conditions.

839 *4.3 Model behaviour*

840 We have analysed some of the model behaviour by changing each of a small number of parameters.
841 This analysis served to confirm expected qualitative outcomes and gain further confidence in the
842 model, and to demonstrate some of the insights that can be derived from an integrated full-cycle
843 model by exploring what-if scenarios. Some scenarios may be hypothetical or impractical to test
844 experimentally in complex pasture systems, making the availability of models particularly valuable as
845 analytical tools.

846 Changing the parasitological history of the pasture by increasing its contamination level at turnout led
847 to earlier peaks in the predicted FEC and worm burden; these time shifts are similar to known peak-
848 shift effects on the prevalence of macroparasites when increasing the force of infection on the host
849 population (Anderson and May, 1985; Woolhouse, 1998). These results also agree with earlier model
850 predictions (Berk et al., 2016b), except the latter contained two successive peaks, while we predicted
851 a single peak during the season and none of the empirical FEC datasets used for validation indicated
852 the occurrence of two peaks. The difference could stem from differing weather or from differing
853 modelling of the parasite FL-stage dynamics, which in Berk et al. (2016b) excluded the influence of
854 precipitation.

855 Likewise, changing in our model the size of the host population by increasing the cattle stocking
856 density led to similar time shifts in the peak excretion of transmission stages and in the peak worm
857 burden. The magnitude of the peak worm burden increased with increasing stocking density in
858 agreement with earlier model predictions (Berk et al., 2016b; Grenfell et al., 1987a). We predicted this
859 same pattern for the peak FEC, which agrees with Berk et al. (2016b) but is opposite to the pattern in

Grenfell et al. (1987a), who highlighted that the worm burden, W, is a more indicative prediction as the FEC is known to be a poor index of parasite burden; although W is more rarely measured for obvious reasons.

Overall, these results confirmed expectations about the behaviour of the model; they also illustrate the importance of measuring L3 on pasture at turnout as some aspects of prediction can be uncertain if this variable is unknown. In addition, in each of the scenarios above there were appreciable effects on BW gain, with the differential between BW trajectories reducing by end of season (due to compensatory growth) in the case of differing initial contamination, but with little or no recovery in lost gain in the case of differing stocking densities. Likewise, the levels of L3 herbage contamination converged by the end of season in the first case, but diverged in the case of differing stocking densities. These outcomes are consistent with lasting effects of higher stocking density (Hansen et al., 1989; Thamsborg et al., 1998) and further confirm expected model behaviour. Overall, the above results highlight that the effects of parasitological history due to grazing in the previous season can be transient, while those of more intense grazing can dominate and be long lasting.

Exploring a set of simple drug treatment strategies, we obtained the following results. First, implementing a single anthelmintic treatment, the model predicted that the optimal application is at an intermediate time after turnout, e.g. 4 weeks, rather than immediately on turnout or later.in the season. This choice is based on multiple criteria: it led to the highest cumulative BW gain and to lower cumulative parasite burden and parasite excretion by the host and thus to potentially lower risk of clinical disease; on the other hand, herbage contamination was comparable to that in the late treatment. This outcome agrees with the expectation that delaying treatment to midseason allows the development of immunity and leads to better parasite control in the long run, while curbing the delay pre-empts the onset of parasite-induced anorexia and leads to better performance. Second, implementing treatment at turnout, the model predicted that the best timing for application of a second treatment is within a time window of 5 to 7 weeks after turnout, rather than immediately after

885 the end of the first treatment at 3 weeks after turnout. This strategy led to a lower level of herbage
886 contamination carried over to the next season and to lower cumulative parasite burden, although it
887 did not lead to significant differences in performance. These treatment scenarios were illustrative and
888 not chosen to mimic specific treatment regimens, although administration of persistent anthelmintic
889 formulations early in the grazing season tend to be favoured due to their strong suppression of egg
890 outputs and consequently of L3 levels. This strategy, however, has been posited to slow the acquisition
891 of immunity (Vercruysse et al., 1994) and could therefore be counterproductive. Overall, these results
892 illustrate the usefulness of a full-cycle epidemiological model for analysing and choosing treatment
893 and management strategies, in particular accounting for performance and not only parasitological
894 outcomes.

895 The predicted effective reproduction number, R_e, exhibited a similar pattern across the empirical
896 studies and the model behaviour analyses: very large initial values, a rapid decline due to the limiting
897 effects of acquired immunity and density dependency, followed by narrow-ranged variation nearly
898 containing the value of 1. We interpret this pattern as reassuring. First, across a range of differing
899 parasitological, host and weather conditions, it agrees with the expectation that the parasite
900 populations will have converged to a state of quasi stability superimposed by short-term fluctuations
901 due to variable host response, weather and seasonal climate. Second, this result supports, rather than
902 questions the consistency of the parameters of the host and free-living model components that we
903 have attempted to integrate into a full-cycle model. Note that such consistency is not automatic as
904 several parameters have been estimated independently.

905 *4.4 Model assumptions and extensions*

906 The model makes several simplifying assumptions already stated. One of the assumptions was that,
907 to first approximation, the growth rate and DM content of the grass biomass did not vary with the
908 weather and throughout the season. Such dependency could be included; however, a fuller account
909 of environmental influence may involve further variables such as soil moisture saturation, and in turn

910 soil type and topography, as well as management factors in relation to grass cultivar and fertiliser
911 application. These refinements go beyond our current purpose and would require substantial
912 empirical support. The current constant rate of grass growth is the average of empirical records from
913 the location and period of the Baseline system (Table 3), but we expect variation in grass growth would
914 have only a mild effect on the transmission rate β (Eq. (29)) . The model also did not include the arrest
915 or hypobiosis of parasitic larval stages and their subsequent re-emergence (Armour, 1980; Michel et
916 al., 1976; Smith and Grenfell, 1985), although this would become relevant only towards the end of the
917 FGS and beyond. Nevertheless, the higher late-season levels of L3 predicted under some scenarios
918 could drive important epidemiological consequences, for example by causing higher risk of type II
919 ostertagiosis through the re-emergence of arrested larvae, or by increasing the levels of pasture
920 contamination in the following season through increased L3 emergence or L3 overwintering on
921 pasture. The model could be extended to include hypobiosis, for example if applied to cattle in
922 subsequent grazing seasons. The consequences of parasite exposure for immunity in older age classes
923 could also be explored in an extended model, including the application of targeted treatment
924 approaches in herds with differing levels of immunity (Ravinet et al., 2017). The model assumed the
925 animals were under thermal neutrality by considering maintenance requirements that did not vary
926 with temperature. The model can be extended to include thermal variation in intake, which is
927 expected to be a very small fraction under varying moderate ambient temperature, but could increase
928 in magnitude under climate warming scenarios.

929 The model describes the dynamics of an average animal and characterises the grazing population
930 through its stocking density. In particular, the model does not include genetic and phenotypic
931 variation. In fact, Smith and Guerrero (1993) have suggested that host heterogeneity in parasite load
932 can be ignored in models aiming to evaluate control strategies that treat all animals in the same way.
933 However, individual-based approaches have been evaluated for sheep (Louie et al., 2005) and cattle
934 (Berk et al., 2016b). The current model could be extended to explore optimal strategies for targeted
935 selected treatments based on individual infection or performance status (Charlier et al., 2014;

936 Höglund et al., 2013; Merlin et al., 2017). Such host heterogeneity provides one of the mechanisms
937 thought to generate the observed aggregation in parasite load and FEC among hosts, the other being
938 the observed aggregation of L3 on pasture (Anderson and Gordon, 1982; Cornell et al., 2004). An
939 alternative, empirical way of accounting for the latter is to make the number of ingested L3 a random
940 variable with an empirical overdispersed distribution such as the negative binomial (Berk et al., 2016b;
941 Smith and Guerrero, 1993) (we took this approach when comparing predictions with empirical data
942 but not in the inherent parasite dynamics). Alternatively, individual-based formulations with
943 stochastic dynamics and spatially-heterogeneous exposure allow both forms of aggregation to be
944 linked mechanistically (Cornell, 2005; Cornell et al., 2004; Fox et al., 2013), but are usually applied to
945 simpler representations of the GIN cycle for tractability (Smith and Grenfell, 1994), and the current
946 addition of weather-driven variation will account for part of the system's dynamic stochasticity. The
947 inclusion of aggregation would strengthen the evaluation of control strategies further when it is
948 relevant to account for heterogeneity in the parasite population; it is expected to influence the
949 dynamics of invading anthelmintic-resistant strains and persisting non-resistant refugia (Cornell, 2005;
950 van Wyk, 2001). Due to aggregation, and other factors already discussed, observations of L3 on
951 herbage in the empirical studies (where reported) are uncertain; its potential effect could have been
952 evaluated by generating distributions of predictions based on an assumed range of input values; these
953 would be expected to include the data in the validation exercise. Sensitivity to uncertainty in other
954 input parameters could be tackled similarly. Taking such an approach would have added an extra layer
955 of complexity to the results, while sensitivity to such factors can be assessed already from the results
956 of the model behaviour study.

957 Finally, as we already discussed extensively, the model was designed for infection by a single-parasite,
958 i.e. *O. ostertagi*, although it was applied to co-infections for reasons explained. This is the case of most
959 models developed for specific GIN infections. Our results, however, supported the application to co-
960 infections by *O. ostertagi* and *C. oncophora* in the empirical studies considered here. A future
961 challenge is to extend such nonlinear models to account explicitly for co-infection. Generic models

962 investigating the implications of parasite co-infection have, for tractability, assumed unspecific host
963 responses to parasite burdens and thus that parasite species did not interact directly (Dobson and
964 Roberts, 1994), but there have been theoretical attempts at including such effects (Bottomley et al.,
965 2005). However, currently, there is little knowledge about which responses would be interacting and
966 how; therefore, more empirical study on GIN co-infection is needed.

967 *4.5 Conclusions*

968 We developed a model of the full life-cycle of *O. ostertagi* that for the first time also incorporates grass
969 and animal growth and data-driven environmental effects on infective larval availability, in addition
970 to host immunity. The model was able to reproduce expected patterns and scales of host growth and
971 parasite dynamics in first season grazing cattle, and closely matched observed results in published
972 studies without the need for model fitting. Exploration of initial pasture conditions, stocking density
973 and treatment scenarios showed that the model can be used to predict the effects of management
974 and climate on infection patterns. Future application could include optimisation of intervention
975 strategies under rapidly changing climate and advancing anthelmintic resistance.

976

977 **Acknowledgements**

978 This research was supported by funding from UK Research and Innovation through grant
979 BB/R010250/1. JANF was also supported in part by the Scottish Government's Rural and Environment
980 Science and Analytical Services (RESAS). The funders had no role in study design, model development,
981 data collection and analysis, decision to publish, or preparation of the manuscript.

982

983 **Declaration of interest**

984 None to declare.

CRediT authorship contribution statement

Joao A. N. Filipe: Conceptualisation, Funding acquisition, Data curation, Formal analysis, Methodology, Project Administration, Software, Validation, Visualisation, Writing – original draft, Writing - review & editing. **Ilias Kyriazakis:** Conceptualisation, Funding acquisition, Project Administration, Validation, Writing – review & editing. **Christopher McFarland:** Investigation, Validation, Writing - review & editing. **Eric R. Morgan:** Conceptualisation, Funding acquisition, Project Administration, Resources, Validation, Writing - review & editing.

Research data for this article

Data that were used to perform the study are publicly available or stated within the main text and in the Supplementary data. Code for the model is available (Filipe, 2022).

Appendix A. Supplementary data

Supplementary data to this article can be found online at xxx

Supplementary data 1

Text S1: Derivation of new model parameters: Cost of maintenance, C_{maint}

Text S2: Derivation of new model parameters: Cost of acquired immunity resources, C_{l1} and C_{l2}

Text S3: Gastrointestinal tract capacity

Text S4: Body weight drop at turnout

Supplementary data 2

Table S1: Parasite free-living stages: environmental dependency

Table S2: Parasite free-living stages: initial state

Supplementary data 3

Figure S1: Weather data used in all studies

Figure S2: Rate of transmission β

References

Anderson, R.C., 2000. Order Strongylida (the Burrsate Nematodes), Nematode Parasites of Vertebrates: Their Development and Transmission. CABI Pub., Wallingford, Oxon, UK; New York, NY, pp. 96–98.

Anderson, R.M., Gordon, D.M., 1982. Processes influencing the distribution of parasite numbers within host populations with special emphasis on parasite-induced host mortalities. Parasitology 85, 373-398.

Anderson, R.M., May, R.M., 1978. Regulation and Stability of Host-Parasite Population Interactions: I. Regulatory Processes. Journal of Animal Ecology 47, 219-247.

Anderson, R.M., May, R.M., 1985. Herd immunity to helminth infection and implications for parasite control. Nature 315, 493-496.

Anderson, R.M., May, R.M., 1992. Infectious diseases of humans : dynamics and control. Oxford university press, Oxford [etc.].

Archer, J.A., Arthur, P.F., Herd, R.M., Parnell, P.F., Pitchford, W.S., 1997. Optimum postweaning test for measurement of growth rate, feed intake, and feed efficiency in British breed cattle. Journal of animal science 75, 2024-2032.

Armour, J., 1980. The epidemiology of helminth disease in farm animals. Veterinary parasitology 6, 7-46.

1031 Balch, C.C., Line, C., 1957. 648. Weight Changes in grazing cows. Journal of Dairy Research 24, 11-19.

1032 Basripuzi, N.H., Sharma, R.S.K., Norhadila, Z., Shahar, Z.S., Nor-Dilaila, M.S., Mustapha, M.S.,

1033 Kolandaiveloo, V., Ruviniyia, K., Matthews, L., 2020. Interaction between abomasal blood feeder

1034 Haemonchus contortus and intestinal mucosal browser Trichostrongylus colubriformis during co-

1035 infection in Boer goats. Veterinary parasitology 287, 109274.

1036 Bell, S.L., Thomas, R.J., Ferber, M.T., 1988. Feed intake of grazing calves exposed to trichostrongyle

1037 infection and treated with the morantel sustained release bolus. Veterinary parasitology 28, 125-135.

1038 Berk, Z., Bishop, S.C., Forbes, A.B., Kyriazakis, I., 2016a. A simulation model to investigate interactions

1039 between first season grazing calves and Ostertagia ostertagi. Veterinary parasitology 226, 198-209.

1040 Berk, Z., Laurenson, Y.C., Forbes, A.B., Kyriazakis, I., 2016b. A stochastic model to investigate the

1041 effects of control strategies on calves exposed to Ostertagia ostertagi. Parasitology 143, 1755-1772.

1042 Bines, J.A., Broster, W.H., Sutton, J.D., Broster, V.J., Napper, D.J., Smith, T., Siviter, J.W., 2009. Effect

1043 of amount consumed and diet composition on the apparent digestibility of feed in cattle and sheep.

1044 The Journal of Agricultural Science 110, 249-259.

1045 Bishop, S.C., Stear, M.J., 1997. Modelling responses to selection for resistance to gastro-intestinal

1046 parasites in sheep. Animal Science 64, 469-478.

1047 Bottomley, C., Isham, V., Basáñez, M.G., 2005. Population biology of multispecies helminth infection:

1048 interspecific interactions and parasite distribution. Parasitology 131, 417-433.

1049 Cain, J.L., Peters, K.T., Suri, P., Roher, A., Rutledge, M.H., Nielsen, M.K., 2021. The effect of analyst

1050 training on fecal egg counting variability. Parasitology research 120, 1363-1370.

1051 Carstens, G.E., Johnson, D.E., Ellenberger, M.A., Tatum, J.D., 1991. Physical and chemical components

1052 of the empty body during compensatory growth in beef steers. Journal of animal science 69, 3251-

1053 3264.

1054 Charlier, J., Höglund, J., Morgan, E.R., Geldhof, P., Vercruysse, J., Claerebout, E., 2020a. Biology and

1055 epidemiology of gastrointestinal nematodes in cattle. The Veterinary clinics of North America. Food

1056 animal practice 36, 1-15.

1057 Charlier, J., Morgan, E.R., Rinaldi, L., van Dijk, J., Demeler, J., Höglund, J., Hertzberg, H., Van Ranst, B.,
1058 Hendrickx, G., Vercruysse, J., Kenyon, F., 2014. Practices to optimise gastrointestinal nematode control
1059 on sheep, goat and cattle farms in Europe using targeted (selective) treatments. Vet Rec 175, 250-255.
1060 Charlier, J., Rinaldi, L., Musella, V., Ploeger, H.W., Chartier, C., Vineer, H.R., Hinney, B., von Samson-
1061 Himmelstjerna, G., Băcescu, B., Mickiewicz, M., Mateus, T.L., Martinez-Valladares, M., Quealy, S.,
1062 Azaizeh, H., Sekovska, B., Akkari, H., Petkevicius, S., Hektoen, L., Höglund, J., Morgan, E.R., Bartley,
1063 D.J., Claerebout, E., 2020b. Initial assessment of the economic burden of major parasitic helminth
1064 infections to the ruminant livestock industry in Europe. Preventive Veterinary Medicine 182, 105103.
1065 Churcher, T.S., Filipe, J.A.N., Basanez, M.G., 2006. Density dependence and the control of helminth
1066 parasites. Journal of Animal Ecology 75, 1313-1320.
1067 Colucci, P.E., Chase, L.E., Van Soest, P.J., 1982. Feed intake, apparent diet digestibility, and rate of
1068 particulate passage in dairy cattle [Nutrient utilization]. v. 65.
1069 Coop, R.L., Kyriazakis, I., 1999. Nutrition–parasite interaction. Veterinary parasitology 84, 187-204.
1070 Coop, R.L., Sykes, A.R., Angus, K.W., 1977. The effect of a daily intake of Ostertagia circumcincta larvae
1071 on body weight, food intake and concentration of serum constituents in sheep. Research in veterinary
1072 science 23, 76-83.
1073 Coop, R.L., Sykes, A.R., Angus, K.W., 1982. The effect of three levels of intake of Ostertagia
1074 Circumcincta Larvae on growth rate, food intake and body composition of growing lambs. The Journal
1075 of Agricultural Science 98, 247-255.
1076 Cornell, S., 2005. Modelling nematode populations: 20 years of progress. Trends in Parasitology 21,
1077 542-545.
1078 Cornell, S.J., Isham, V.S., Grenfell, B.T., 2004. Stochastic and spatial dynamics of nematode parasites
1079 in farmed ruminants. Proc Biol Sci 271, 1243-1250.
1080 Cornes, R.C., van der Schrier, G., van den Besselaar, E.J.M., Jones, P.D., 2018. An Ensemble Version of
1081 the E-OBS Temperature and Precipitation Data Sets. Journal of Geophysical Research: Atmospheres
1082 123, 9391-9409.

1083 Denwood, M.J., Love, S., Innocent, G.T., Matthews, L., McKendrick, I.J., Hillary, N., Smith, A., Reid,
1084 S.W.J., 2012. Quantifying the sources of variability in equine faecal egg counts: Implications for
1085 improving the utility of the method. Veterinary parasitology 188, 120-126.
1086 Dimander, S.-O., Höglund, J., Uggla, A., Spörndly, E., Waller, P.J., 2003. Evaluation of gastro-intestinal
1087 nematode parasite control strategies for first-season grazing cattle in Sweden. Veterinary parasitology
1088 111, 193-209.
1089 Dobson, A., Roberts, M., 1994. The population dynamics of parasitic helminth communities.
1090 Parasitology 109 Suppl, S97-108.
1091 Doeschl-Wilson, A.B., Vagenas, D., Kyriazakis, I., Bishop, S.C., 2008. Exploring the assumptions
1092 underlying genetic variation in host nematode resistance (Open Access publication). Genetics,
1093 selection, evolution : GSE 40, 241-264.
1094 Dorny, P., Claerebout, E., Vercruysse, J., Hilderson, H., Huntley, J.F., 1997. The influence of a Cooperia
1095 oncophora priming on a concurrent challenge with Ostertagia ostertagi and C. oncophora in calves.
1096 Veterinary parasitology 70, 143-151.
1097 EBLEX, 2013. English Beef and Lamb Executive. Planning Grazing Strategies for Better Returns. UK:
1098 http://www.eblex.org.uk/wp/wp-content/uploads/2013/06/Manual-8-Planning-
1099 grazing_strategies_200313.pdf , Accesses: July 2016.
1100 Filipe, J.A.N., 2022. Epidemiological model of GIN infection in grazing cattle, , URL:
1101 https://github.com/JAN-Filipe/Epidemiological-model-of-GIN-infection-in-grazing-cattle.
1102 Filipe, J.A.N., Boussinesq, M., Renz, A., Collins, R.C., Vivas-Martinez, S., Grillet, M.E., Little, M.P.,
1103 Basanez, M.G., 2005. Human infection patterns and heterogeneous exposure in river blindness.
1104 Proceedings of the National Academy of Sciences of the United States of America 102, 15265-15270.
1105 Filipe, J.A.N., Leinonen, I., Kyriazakis, I., 2018. The quantitative principles of animal growth, in: Paul
1106 Moughan, W.H. (Ed.), Feed Evaluation Science. Wageningen Academic Publishers, The Netherlands
1107 pp. 387-422.
1108 Forbes, A.B., 2020. Parasites of cattle and sheep : a practical guide to their biology and control.

1109 Forni, S., Piles, M., Blasco, A., Varona, L., Oliveira, H.N., Lôbo, R.B., Albuquerque, L.G., 2009.
1110 Comparison of different nonlinear functions to describe Nelore cattle growth. Journal of animal
1111 science 87, 496-506.
1112 Fox, M.T., 1993. Pathophysiology of infection with Ostertagia ostertagi in cattle. Veterinary
1113 parasitology 46, 143-158.
1114 Fox, M.T., Gerrelli, D., Pitt, S.R., Jacobs, D.E., Gill, M., Gale, D.L., 1989. Ostertagia ostertagi infection in
1115 the calf: effects of a trickle challenge on appetite, digestibility, rate of passage of digesta and
1116 liveweight gain. Research in veterinary science 47, 294-298.
1117 Fox, N.J., Marion, G., Davidson, R.S., White, P.C.L., Hutchings, M.R., 2013. Modelling Parasite
1118 Transmission in a Grazing System: The Importance of Host Behaviour and Immunity. PLOS ONE 8,
1119 e77996.
1120 González-García, E., Golini, P.O., Hassoun, P., Bocquier, F., Hazard, D., González, L.A., Ingham, A.B.,
1121 Bishop-Hurley, G.J., Greenwood, P.L., 2018. An assessment of Walk-over-Weighing to estimate short-
1122 term individual forage intake in sheep. Animal : an international journal of animal bioscience 12, 1174-
1123 1181.
1124 GrassCheck, 2021. Grass Check GB. Grass Growth and Quality; https://www.grasscheckgb.co.uk/ ,
1125 Accesses: Nov 2021. Centre for Innovation Excellence in Livestock (CIEL).
1126 Greer, A.W., Hamie, J.C., 2016. Relative maturity and the development of immunity to gastrointestinal
1127 nematodes in sheep: an overlooked paradigm? Parasite immunology 38, 263-272.
1128 Grenfell, B.T., 1988. Gastrointestinal nematode parasites and the stability and productivity of intensive
1129 ruminant grazing systems. Philosophical transactions of the Royal Society of London. Series B,
1130 Biological sciences 321, 541-563.
1131 Grenfell, B.T., Smith, G., Anderson, R.M., 1986. Maximum-likelihood estimates of the mortality and
1132 migration rates of the infective larvae of Ostertagia ostertagi and Cooperia oncophora. Parasitology
1133 92 (Pt 3), 643-652.

1134 Grenfell, B.T., Smith, G., Anderson, R.M., 1987a. A mathematical model of the population biology of
1135 Ostertagia ostertagi in calves and yearlings. Parasitology 95 (Pt 2), 389-406.
1136 Grenfell, B.T., Smith, G., Anderson, R.M., 1987b. The regulation of Ostertagia ostertagi populations in
1137 calves: the effect of past and current experience of infection on proportional establishment and
1138 parasite survival. Parasitology 95 (Pt 2), 363-372.
1139 Hansen, J.W., Zajac, A.M., Eversole, D.E., Gerken, H.J., Jr., 1989. The effect of stocking rate and parasite
1140 control on the performance of replacement beef heifers on pasture. Veterinary parasitology 34, 103-
1141 115.
1142 Hart, K.J., Martin, P.G., Foley, P.A., Kenny, D.A., Boland, T.M., 2009. Effect of sward dry matter
1143 digestibility on methane production, ruminal fermentation, and microbial populations of zero-grazed
1144 beef cattle1. Journal of animal science 87, 3342-3350.
1145 Heesterbeek, J.A., Roberts, M.G., 1995. Threshold quantities for helminth infections. Journal of
1146 mathematical biology 33, 415-434.
1147 Henriksen, S.A., Jorgensen, R.J., Nansen, P., Sejrsen, K., Brolund-Larsen, J., Klausen, S., 1976.
1148 Ostertagiasis in calves. I. The effect of control measures on infection levels and body weight gains
1149 during the grazing season in Denmark, [Gastrointestinal helminth infection].
1150 Herlich, H., 1965. Immunity and cross immunity to Cooperia oncophora and Cooperia pectinata in
1151 calves and lambs. American journal of veterinary research 26, 1037-1041.
1152 Hilderson, H., Vercruysse, J., Claerebout, E., De Graaf, D.C., Fransen, J., Berghen, F.P., 1995.
1153 Interactions between Ostertagia ostertagi and Cooperia oncophora in calves. Veterinary parasitology
1154 56, 107-119.
1155 Hodgkinson, J.E., Kaplan, R.M., Kenyon, F., Morgan, E.R., Park, A.W., Paterson, S., Babayan, S.A.,
1156 Beesley, N.J., Britton, C., Chaudhry, U., Doyle, S.R., Ezenwa, V.O., Fenton, A., Howell, S.B., Laing, R.,
1157 Mable, B.K., Matthews, L., McIntyre, J., Milne, C.E., Morrison, T.A., Prentice, J.C., Sargison, N.D.,
1158 Williams, D.J.L., Wolstenholme, A.J., Devaney, E., 2019. Refugia and anthelmintic resistance: Concepts
1159 and challenges. International Journal for Parasitology: Drugs and Drug Resistance 10, 51-57.

1160 Högberg, N., Hessle, A., Lidfors, L., Baltrušis, P., Claerebout, E., Höglund, J., 2021. Subclinical nematode
1161 parasitism affects activity and rumination patterns in first-season grazing cattle. Animal : an
1162 international journal of animal bioscience 15, 100237.
1163 Höglund, J., Dahlström, F., Sollenberg, S., Hessle, A., 2013. Weight gain-based targeted selective
1164 treatments (TST) of gastrointestinal nematodes in first-season grazing cattle. Veterinary parasitology
1165 196, 358-365.
1166 Höglund, J., Hessle, A., Zaralis, K., Arvidsson-Segerkvist, K., Athanasiadou, S., 2018. Weight gain and
1167 resistance to gastrointestinal nematode infections in two genetically diverse groups of cattle.
1168 Veterinary parasitology 249, 88-91.
1169 Houdijk, J.G., Jessop, N.S., Kyriazakis, I., 2001. Nutrient partitioning between reproductive and
1170 immune functions in animals. The Proceedings of the Nutrition Society 60, 515-525.
1171 Johnson, J.R., Carstens, G.E., Krueger, W.K., Lancaster, P.A., Brown, E.G., Tedeschi, L.O., Anderson,
1172 R.C., Johnson, K.A., Brosh, A., 2019. Associations between residual feed intake and apparent nutrient
1173 digestibility, in vitro methane-producing activity, and volatile fatty acid concentrations in growing beef
1174 cattle1. Journal of animal science 97, 3550-3561.
1175 Kao, R.R., Leathwick, D.M., Roberts, M.G., Sutherland, I.A., 2000. Nematode parasites of sheep: a
1176 survey of epidemiological parameters and their application in a simple model. Parasitology 121, 85-
1177 103.
1178 Kaplan, R.M., Vidyashankar, A.N., 2012. An inconvenient truth: global worming and anthelmintic
1179 resistance. Veterinary parasitology 186, 70-78.
1180 Kloosterman, A., 1971. Observations on the epidemiology of trichostrongylosis of calves. Veenman,
1181 Wageningen.
1182 Kloosterman, A., Albers, G.A., van den Brink, R., 1984. Negative interactions between Ostertagia
1183 ostertagi and Cooperia oncophora in calves. Veterinary parasitology 15, 135-150.

1184 Larsson, A., Dimander, S.O., Rydzik, A., A.Uggla, Waller, P.J., Höglund, J., 2007. A 3-year field evaluation
1185 of pasture rotation and supplementary feeding to control parasite infection in first-season grazing
1186 cattle—Dynamics of pasture infectivity. Veterinary parasitology 145, 129-137.
1187 Larsson, A., Dimander, S.O., Rydzik, A., Uggla, A., Waller, P.J., Höglund, J., 2006. A 3-year field
1188 evaluation of pasture rotation and supplementary feeding to control parasite infection in first-season
1189 grazing cattle—Effects on animal performance. Veterinary parasitology 142, 197-206.
1190 Le Jambre, L.F., Dominik, S., Eady, S.J., Henshall, J.M., Colditz, I.G., 2007. Adjusting worm egg counts
1191 for faecal moisture in sheep. Veterinary parasitology 145, 108-115.
1192 Leclerc, M., Dore, T., Gilligan, C.A., Lucas, P., Filipe, J.A.N., 2014. Estimating the Delay between Host
1193 Infection and Disease (Incubation Period) and Assessing Its Significance to the Epidemiology of Plant
1194 Diseases. Plos One 9.
1195 Lello, J., McClure, S.J., Tyrrell, K., Viney, M.E., 2018. Predicting the effects of parasite co-infection
1196 across species boundaries. Proc Biol Sci 285.
1197 Louie, K., Vlassoff, A., Mackay, A., 2005. Nematode parasites of sheep: extension of a simple model to
1198 include host variability. Parasitology 130, 437-446.
1199 Louie, K., Vlassoff, A., Mackay, A.D., 2007. Gastrointestinal nematode parasites of sheep: A dynamic
1200 model for their effect on liveweight gain. International journal for parasitology 37, 233-241.
1201 Mayer, D.G., Butler, D.G., 1993. Statistical validation. Ecological Modelling 68, 21-32.
1202 Merlin, A., Ravinet, N., Madouasse, A., Bareille, N., Chauvin, A., Chartier, C., 2017. Mid-season targeted
1203 selective anthelmintic treatment based on flexible weight gain threshold for nematode infection
1204 control in dairy calves. Animal : an international journal of animal bioscience 12, 1030-1040.
1205 Michel, J.F., 1969. Some observations on the worm burdens of calves infected daily with Ostertagia
1206 ostertagi. Parasitology 59, 575-595.
1207 Michel, J.F., Lancaster, M.B., Hong, C., 1970. Field observations on the epidemiology of parasitic
1208 gastro-enteritis in calves. Research in veterinary science 11, 255-259.

1209 Michel, J.F., Lancaster, M.B., Hong, C., 1973. Inhibition of development: variation within a population
1210 of Ostertagia ostertagi. J Comp Pathol 83, 351-356.
1211 Michel, J.F., Lancaster, M.B., Hong, C., 1976. Observations on the resumed development of arrested
1212 Ostertagia ostertagi in naturally infected yearling cattle. Journal of Comparative Pathology 86, 73-80.
1213 Moore, J.F., 1978. Occurrence of Trichostrongylid Nematodes in Cattle Slurry. Irish Journal of
1214 Agricultural Research 17, 255-266.
1215 Nansen, P., Foldager, J., Hansen, J.W., Henriksen, S.A., Jørgensen, R.J., 1988. Grazing pressure and
1216 acquisition of Ostertagia ostertagi in calves. Veterinary parasitology 27, 325-335.
1217 Nennich, T.D., Harrison, J.H., VanWieringen, L.M., Meyer, D., Heinrichs, A.J., Weiss, W.P., St-Pierre,
1218 N.R., Kincaid, R.L., Davidson, D.L., Block, E., 2005. Prediction of Manure and Nutrient Excretion from
1219 Dairy Cattle. Journal of Dairy Science 88, 3721-3733.
1220 NRC, 1987. Predicting Feed Intake of Food-Producing Animals. The National Academies Press,
1221 Washington, DC.
1222 O'Shaughnessy, J., Earley, B., Mee, J.F., Doherty, M.L., Crosson, P., Barrett, D., de Waal, T., 2015.
1223 Nematode control in suckler beef cattle over their first two grazing seasons using a targeted selective
1224 treatment approach. Irish veterinary journal 68, 13.
1225 Paras, K.L., George, M.M., Vidyashankar, A.N., Kaplan, R.M., 2018. Comparison of fecal egg counting
1226 methods in four livestock species. Veterinary parasitology 257, 21-27.
1227 Ravinet, N., Lehebel, A., Bareille, N., Lopez, C., Chartier, C., Chauvin, A., Madouasse, A., 2017. Design
1228 and evaluation of multi-indicator profiles for targeted-selective treatment against gastrointestinal
1229 nematodes at housing in adult dairy cows. Veterinary parasitology 237, 17-29.
1230 Roberts, M.G., Grenfell, B.T., 1991. The Population Dynamics of Nematode Infections of Ruminants:
1231 Periodic Perturbations as a Model for Management. Mathematical Medicine and Biology: A Journal of
1232 the IMA 8, 83-93.

1233 Rose, H., Wang, T., van Dijk, J., Morgan, E.R., 2015. GLOWORM-FL: A simulation model of the effects
1234 of climate and climate change on the free-living stages of gastro-intestinal nematode parasites of
1235 ruminants. Ecological Modelling 297, 232-245.
1236 Rose Vineer, H., Morgan, E.R., Hertzberg, H., Bartley, D.J., Bosco, A., Charlier, J., Chartier, C.,
1237 Claerebout, E., de Waal, T., Hendrickx, G., Hinney, B., Höglund, J., Ježek, J., Kašný, M., Keane, O.M.,
1238 Martínez-Valladares, M., Mateus, T.L., McIntyre, J., Mickiewicz, M., Munoz, A.M., Phythian, C.J.,
1239 Ploeger, H.W., Rataj, A.V., Skuce, P.J., Simin, S., Sotiraki, S., Spinu, M., Stuen, S., Thamsborg, S.M.,
1240 Vadlejch, J., Varady, M., von Samson-Himmelstjerna, G., Rinaldi, L., 2020a. Increasing importance of
1241 anthelmintic resistance in European livestock: creation and meta-analysis of an open database.
1242 Parasite (Paris, France) 27, 69.
1243 Rose Vineer, H., Verschave, S.H., Claerebout, E., Vercruysse, J., Shaw, D.J., Charlier, J., Morgan, E.R.,
1244 2020b. GLOWORM-PARA: a flexible framework to simulate the population dynamics of the parasitic
1245 phase of gastrointestinal nematodes infecting grazing livestock. International journal for parasitology
1246 50, 133-144.
1247 Roseby, F., 1973. Effects of *Trichostrongylus colubriformis* (Nematoda) on the nutrition and
1248 metabolism of sheep. I. Feed intake, digestion, and utilization. Australian Journal of Agricultural
1249 Research 24, 947-953.
1250 Sandberg, F.B., Emmans, G.C., Kyriazakis, I., 2006. A model for predicting feed intake of growing
1251 animals during exposure to pathogens. Journal of animal science 84, 1552-1566.
1252 Satrija, F., Nansen, P., 1993. Experimental concurrent infections with Ostertagia ostertagi and
1253 Cooperia oncophora in the calf. Research in veterinary science 55, 92-97.
1254 Sauermann, C.W., Leathwick, D.M., 2018. A climate-driven model for the dynamics of the free-living
1255 stages of Cooperia oncophora. Veterinary parasitology 255, 83-90.
1256 Singleton, D.R., Stear, M.J., Matthews, L., 2011. A mechanistic model of developing immunity to
1257 Teladorsagia circumcincta infection in lambs. Parasitology 138, 322-332.

1258 Skuce, P.J., Morgan, E.R., van Dijk, J., Mitchell, M., 2013. Animal health aspects of adaptation to
1259 climate change: beating the heat and parasites in a warming Europe. Animal : an international journal
1260 of animal bioscience 7 Suppl 2, 333-345.
1261 Smith, G., 1990. The population biology of the free-living phase of Haemonchus contortus.
1262 Parasitology 101, 309-316.
1263 Smith, G., 1994. Population biology of the parasitic phase of trichostrongylid nematode parasites of
1264 cattle and sheep. International journal for parasitology 24, 167-178.
1265 Smith, G., 1997. The economics of parasite control: obstacles to creating reliable models. Veterinary
1266 parasitology 72, 437-449.
1267 Smith, G., 2011. Models of macroparasitic infections in domestic ruminants: a conceptual review and
1268 critique. Rev Sci Tech 30, 447-456.
1269 Smith, G., Grenfell, B.T., 1985. The population biology of Ostertagia ostertagi. Parasitology Today 1,
1270 76-81.
1271 Smith, G., Grenfell, B.T., 1994. Modelling of parasite populations: gastrointestinal nematode models.
1272 Veterinary parasitology 54, 127-143.
1273 Smith, G., Grenfell, B.T., Anderson, R.M., 1986. The development and mortality of the non-infective
1274 free-living stages of Ostertagia ostertagi in the field and in laboratory culture. Parasitology 92 (Pt 2),
1275 471-482.
1276 Smith, G., Grenfell, B.T., Anderson, R.M., 1987. The regulation of Ostertagia ostertagi populations in
1277 calves: density-dependent control of fecundity. Parasitology 95 (Pt 2), 373-388.
1278 Smith, G., Guerrero, J., 1993. Mathematical models for the population biology of Ostertagia ostertagi
1279 and the significance of aggregated parasite distributions. Veterinary parasitology 46, 243-257.
1280 Sykes, A.R., Poppi, D.P., Elliot, D.C., 2009. Effect of concurrent infection with Ostertagia circumcincta
1281 and Trichostrongylus colubriformis on the performance of growing lambs consuming fresh herbage.
1282 The Journal of Agricultural Science 110, 531-541.

1283 Symons, L.E., 1985. Anorexia: occurrence, pathophysiology, and possible causes in parasitic infections.
1284 Advances in parasitology 24, 103-133.
1285 Szyszka, O., Tolkamp, B.J., Edwards, S.A., Kyriazakis, I., 2013. Do the changes in the behaviours of cattle
1286 during parasitism with Ostertagia ostertagi have a potential diagnostic value? Veterinary parasitology
1287 193, 214-222.
1288 Taylor, L.M., Parkins, J.J., Armour, J., Holmes, P.H., Bairden, K., Ibarra-Silva, A.M., Salman, S.K.,
1289 McWilliam, P.N., 1989. Pathophysiological and parasitological studies on Ostertagia ostertagi
1290 infections in calves. Research in veterinary science 46, 218-225.
1291 Thamsborg, S.M., Jørgensen, R.J., Nansen, P., 1998. Internal parasitism of steers grazing extensively at
1292 different stocking rates. Acta veterinaria Scandinavica 39, 311-323.
1293 Tompkins, D.M., Dobson, A.P., Arneberg, P., Begon, M.E., Cattadori, I., Greenman, J.V., Heesterbeek,
1294 J.A.P., Hudson, P., Newborn, D., 2001. Parasites and host population dynamics, in: Hudson, P.J., Rizzoli,
1295 A., Grenfell, B.T., Heesterbeek, J.A.P., Dobson, A.P. (Eds.), The Ecology of Wildlife Diseases. Oxford
1296 University Press, New York, pp. 45-62.
1297 Tontini, J.F., Espírito Candal Poli, C.H., da Silva Hampel, V., Fajardo, N.M., Afonso Martins, A., Pelegrine
1298 Minho, A., Muir, J.P., 2019. Dispersal and concentration of sheep gastrointestinal nematode larvae on
1299 tropical pastures. v. 174.
1300 UGS, 2010. Ulster Grassland Society 2010 Grazing Management Booklet , Accesses: Nov 2021. Ulster
1301 Grassland Society.
1302 Vagenas, D., Bishop, S.C., Kyriazakis, I., 2007. A model to account for the consequences of host
1303 nutrition on the outcome of gastrointestinal parasitism in sheep: logic and concepts. Parasitology 134,
1304 1263-1277.
1305 van Wyk, J.A., 2001. Refugia--overlooked as perhaps the most potent factor concerning the
1306 development of anthelmintic resistance. The Onderstepoort journal of veterinary research 68, 55-67.
1307 Vercruysse, J., Charlier, J., Van Dijk, J., Morgan, E.R., Geary, T., von Samson-Himmelstjerna, G.,
1308 Claerebout, E., 2018. Control of helminth ruminant infections by 2030. Parasitology 145, 1655-1664.

1309 Vercruysse, J., Hilderson, H., Claerebout, E., 1994. Effect of chemoprophylaxis on immunity to
1310 gastrointestinal nematodes in cattle. Parasitology today (Personal ed.) 10, 129-132.
1311 Verschave, S.H., Charlier, J., Rose, H., Claerebout, E., Morgan, E.R., 2016a. Cattle and Nematodes
1312 Under Global Change: Transmission Models as an Ally. Trends in Parasitology 32, 724-738.
1313 Verschave, S.H., Levecke, B., Duchateau, L., Vercruysse, J., Charlier, J., 2015. Measuring larval
1314 nematode contamination on cattle pastures: Comparing two herbage sampling methods. Veterinary
1315 parasitology 210, 159-166.
1316 Verschave, S.H., Rose, H., Morgan, E.R., Claerebout, E., Vercruysse, J., Charlier, J., 2016b. Modelling
1317 Cooperia oncophora: Quantification of key parameters in the parasitic phase. Veterinary parasitology
1318 223, 111-114.
1319 Verschave, S.H., Vercruysse, J., Claerebout, E., Rose, H., Morgan, E.R., Charlier, J., 2014. The parasitic
1320 phase of Ostertagia ostertagi: quantification of the main life history traits through systematic review
1321 and meta-analysis. International journal for parasitology 44, 1091-1104.
1322 Williams, C.B., Keele, J.W., Waldo, D.R., 1992. A computer model to predict empty body weight in
1323 cattle from diet and animal characteristics. Journal of animal science 70, 3215-3222.
1324 Woolhouse, M.E., 1998. Patterns in parasite epidemiology: the peak shift. Parasitology today (Personal
1325 ed.) 14, 428-434.

1326

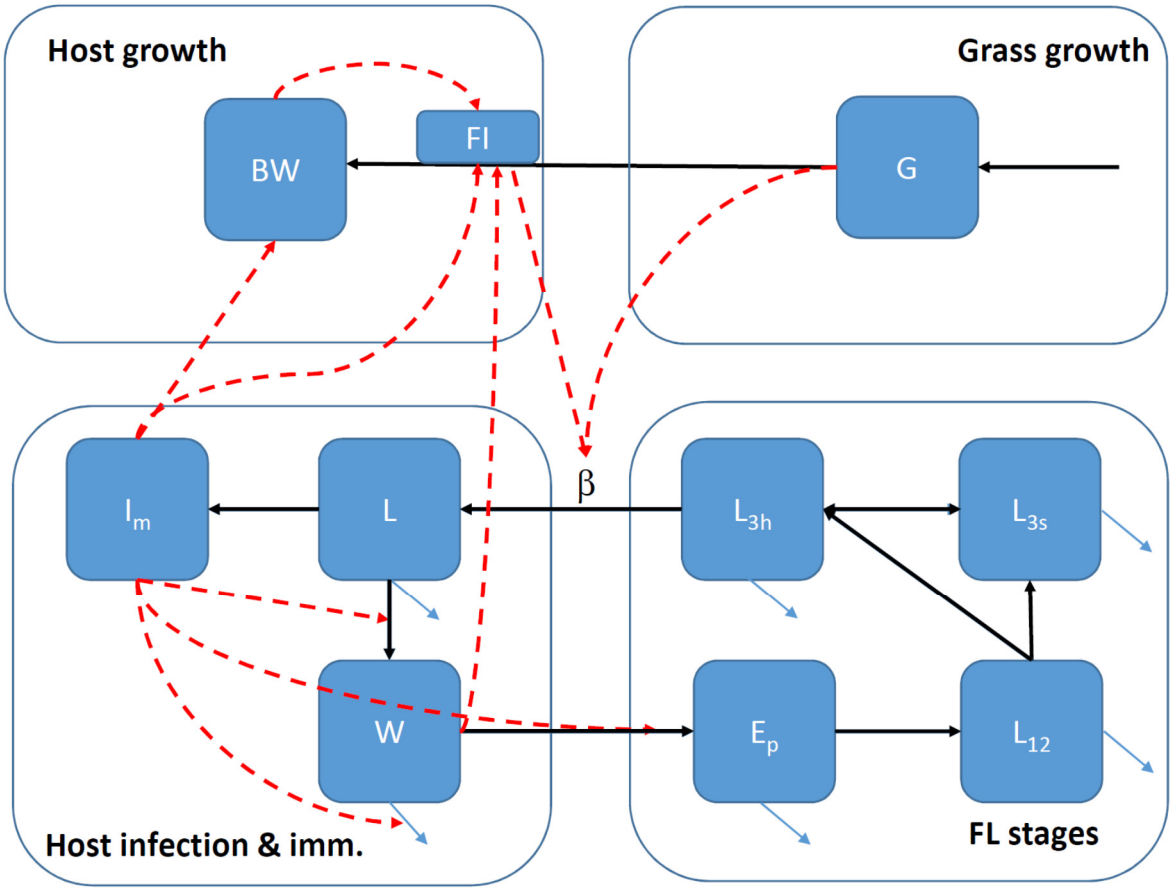

Fig. 1. Structure of the full-cycle model of GIN transmission. The model comprises four sub-models representing: host growth; grass growth; host infection and the development of immunity; and the free living (FL) parasite stages. The details of each sub-model are given in the text, Sections 2.2 to 2.5. Squares: state variables. Arrows: flow or transition (black), mortality (blue), influence (red).

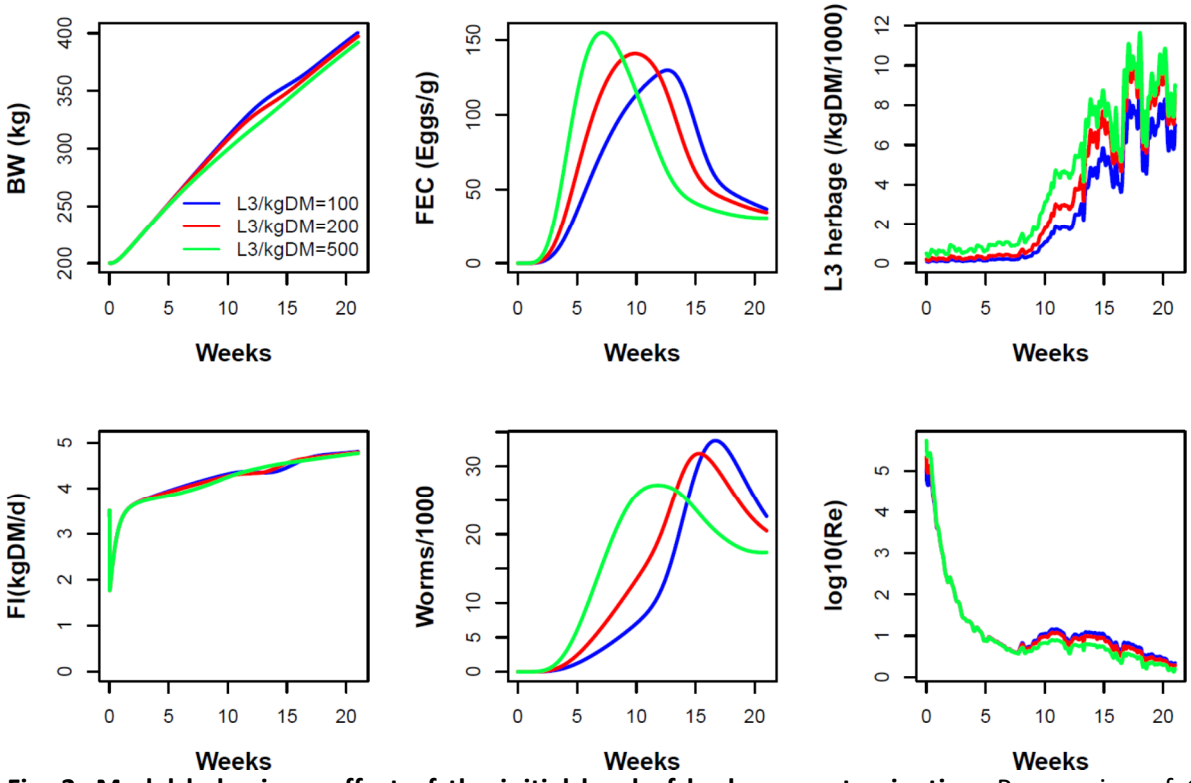

Fig. 2. Model behaviour: effect of the initial level of herbage contamination. Progression of *O. ostertagi* infection during the grazing season of the baseline herd and grazing system under differing initial concentrations of L3 on herbage, 100, 200, 500 larvae/kg dry matter (DM). Traits shown: body weight (BW), faecal egg count (FEC) in wet faeces, density of L3 on dry herbage, daily feed intake (FI), number of adult worms, and logarithm of the effective reproduction number R_e.

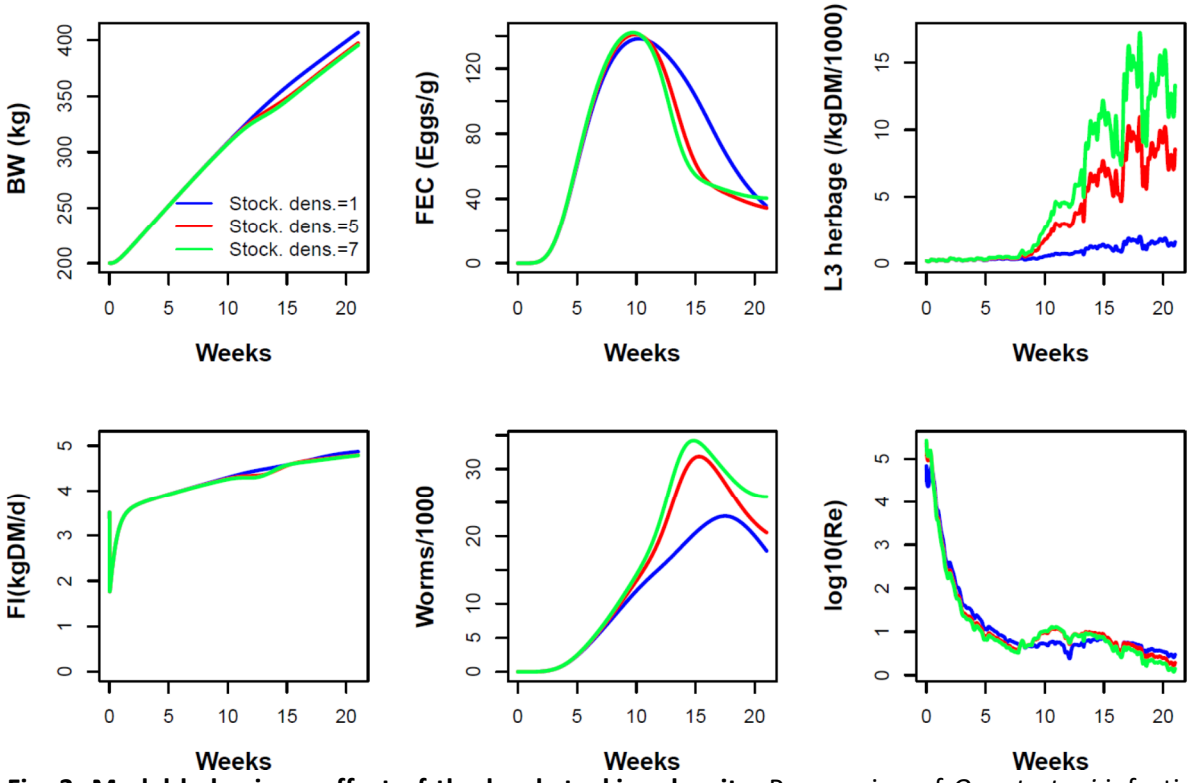

Fig. 3. Model behaviour: effect of the herd stocking density. Progression of *O. ostertagi* infection during the grazing season of the baseline herd and grazing system under differing herd stocking densities, N_h = 1, 5, and 7 animals/ha. Traits shown: body weight (BW), faecal egg count (FEC) in wet faeces, density of L3 on dry herbage, daily feed intake (FI), number of adult worms, and logarithm of the effective reproduction number R_e.

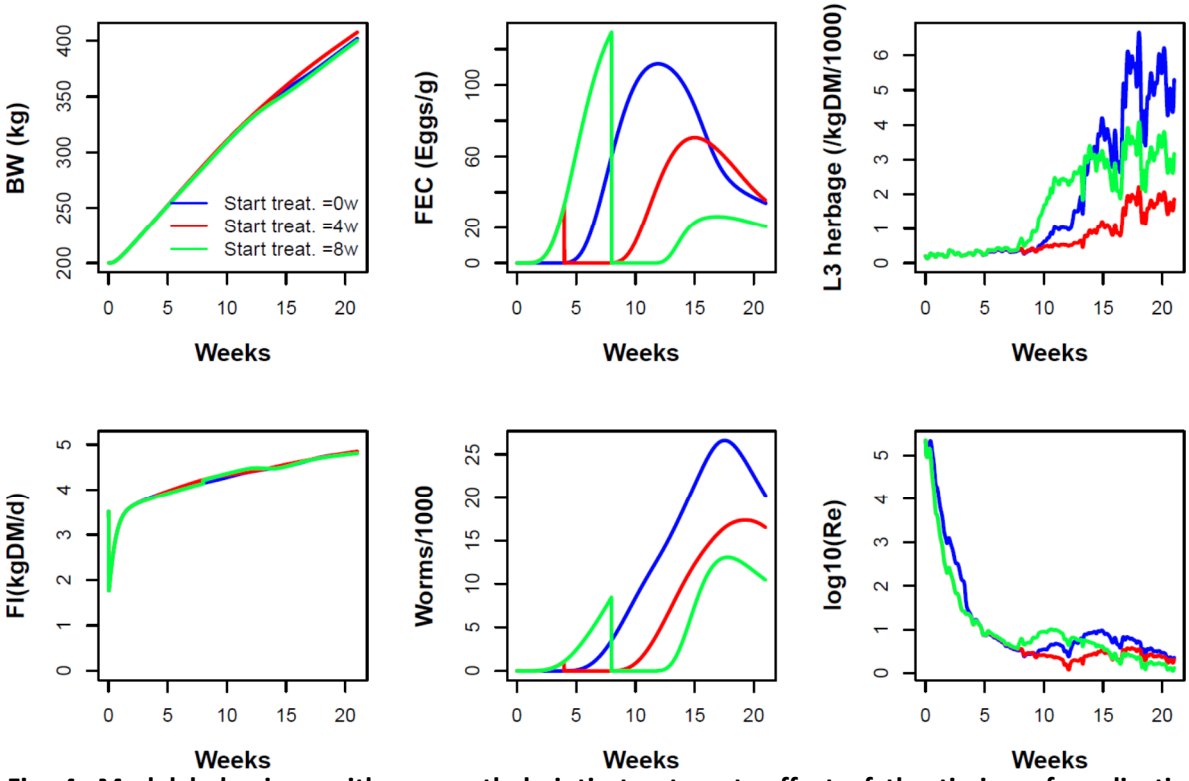

1341 **Fig. 4. Model behaviour with one anthelmintic treatment: effect of the timing of application.**

1342 Progression of *O. ostertagia* infection during the grazing season of the baseline herd and grazing

1343 system with one round of anthelmintic treatment with differing times of application, 0, 4 and 8 weeks

1344 after turnout (see Section 2.7.3 for details on drug treatment). Traits shown: body weight (BW), faecal

1345 egg count (FEC) in wet faeces, density of L3 on dry herbage, daily feed intake (FI), number of adult

1346 worms, and logarithm of the effective reproduction number R_e.

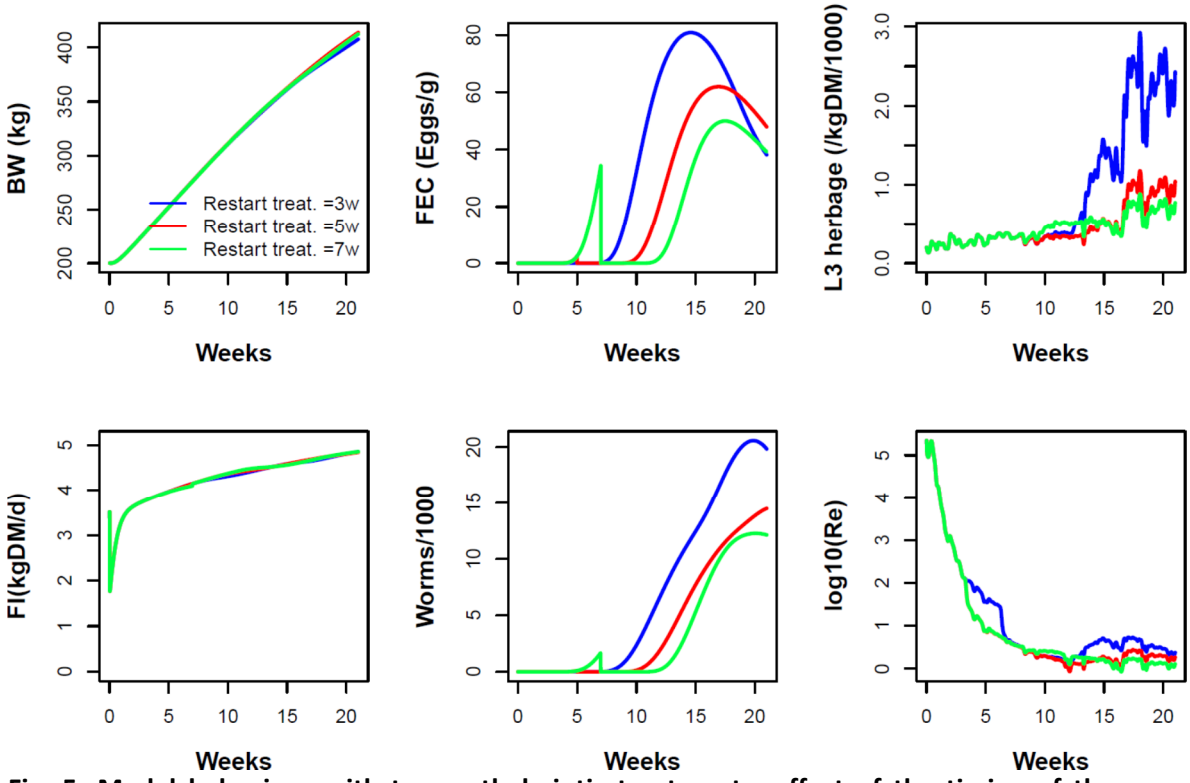

Fig. 5. Model behaviour with two anthelmintic treatments: effect of the timing of the second treatment. Progression of *O. ostertagi* infection during the grazing season of the baseline herd and grazing system with a first round of anthelmintic treatment at turnout but differing in the time of application of the second round, at 3, 5, and 7 weeks after turnout. Drug efficacy is maintained for 3 weeks (see text for details on drug treatment). Traits shown: body weight (BW), faecal egg count (FEC) in wet faeces, density of L3 on dry herbage, daily feed intake (FI), number of adult worms, and logarithm of the effective reproduction number R_e.

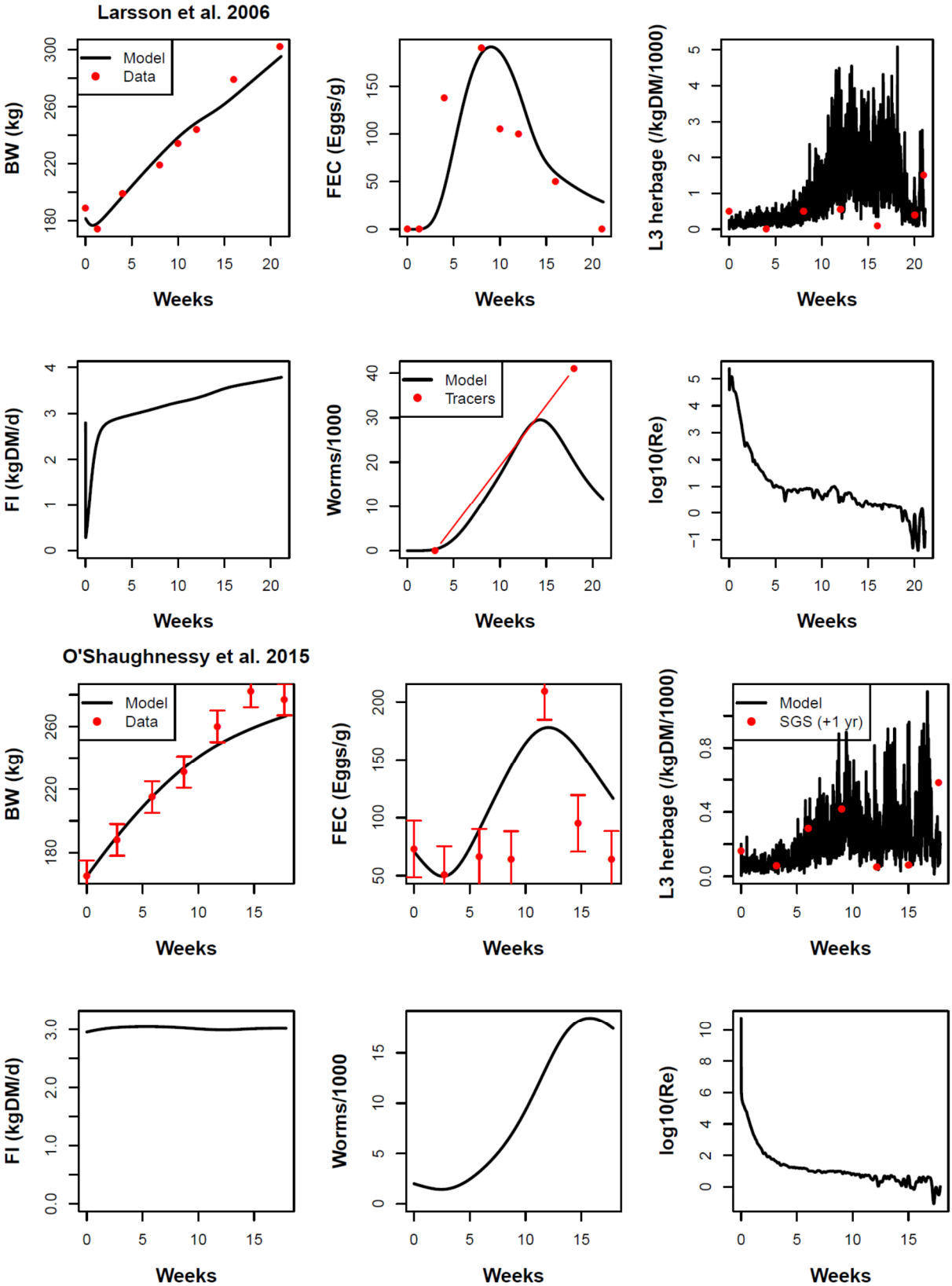

Fig. 6. Model comparison with studies involving natural infection of cattle: Larsson et al. (2006) (rows 1 and 2) and O'Shaughnessy et al. (2015) (rows 3 and 4). Traits shown: body weight (BW), faecal egg count (FEC) in wet faeces, density of L3 on dry herbage, daily feed intake (FI), number of adult worms, and logarithm of the effective reproduction number R_e. Animals were infected with a mixture of *O. ostertagi* and *C. oncophora*. The results of the statistical tests are given in Table 6.

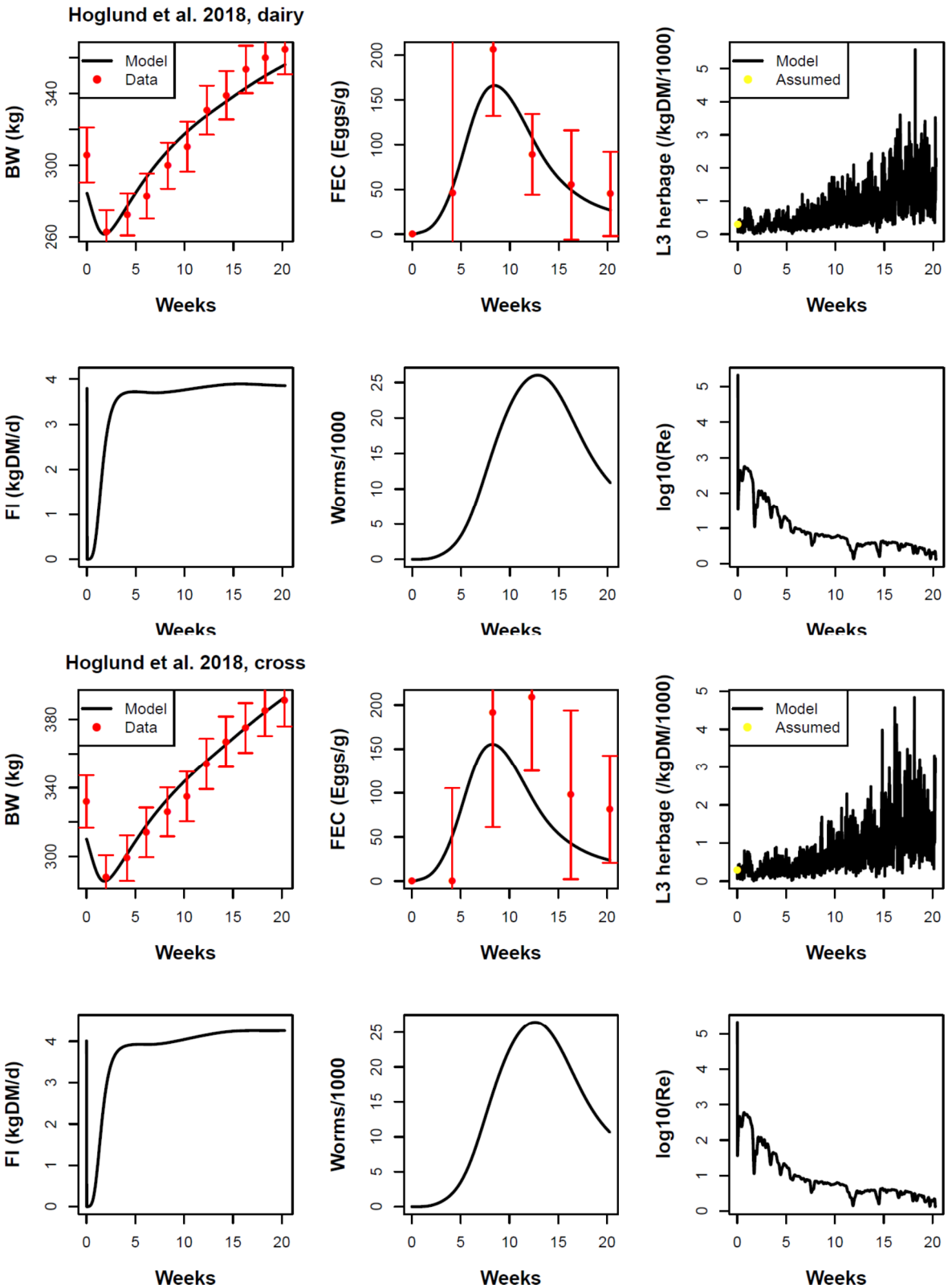

Fig. 7. Model comparison with studies providing a low parasite dose pre-turnout followed by natural infection: Höglund et al. (2018) dairy breed (rows 1 and 2) and cross breed (rows 3 and 4). Traits shown: body weight (BW), faecal egg count (FEC) in wet faeces, density of L3 on dry herbage, daily feed intake (FI), number of adult worms, and logarithm of the effective reproduction number R_e. The parasite dose at turnout was a 5000 even mixture of *O. ostertagi* and *C. oncophora*. The results of the statistical tests are given in Table 6.

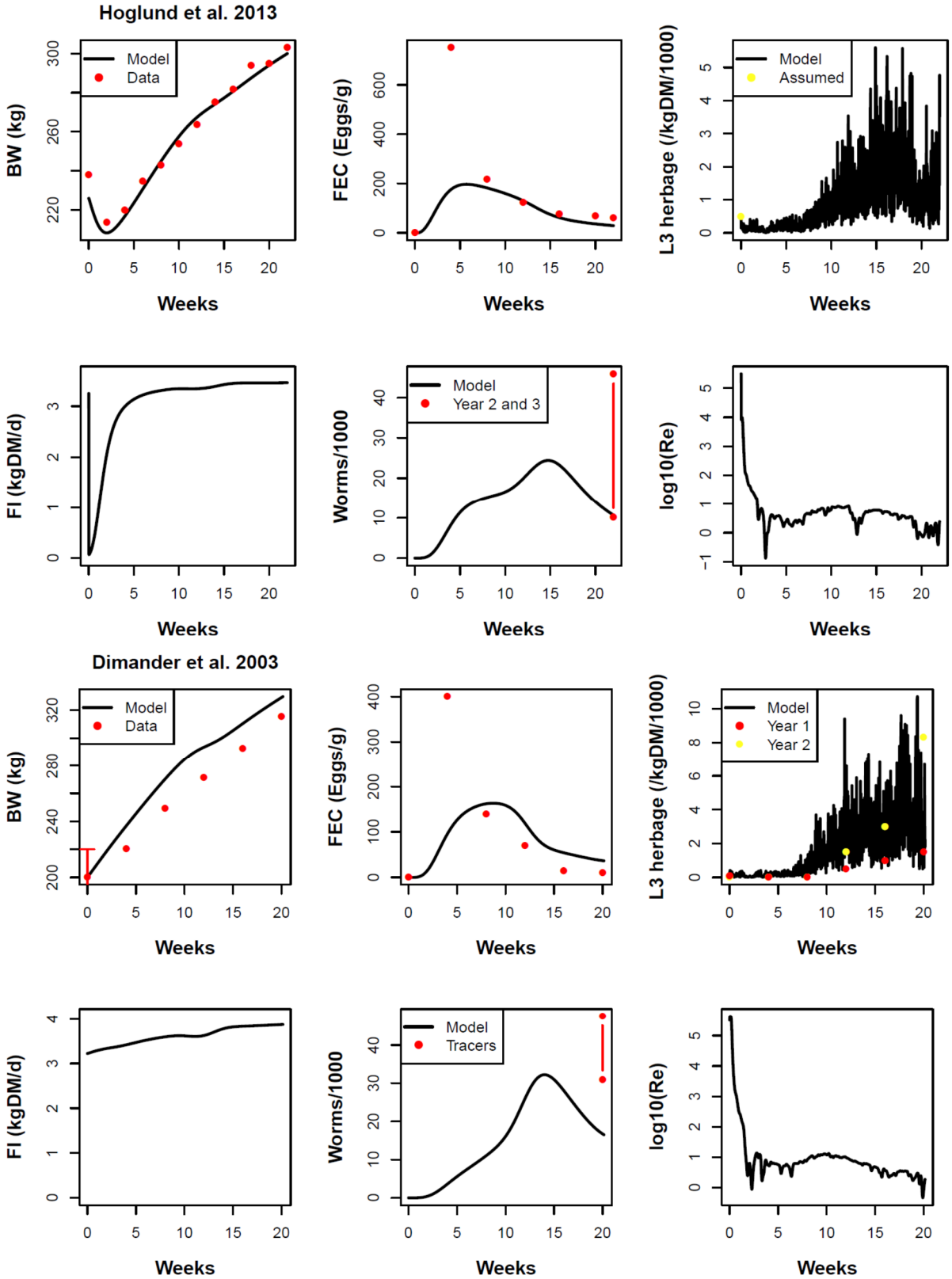

Fig. 8. Model comparison with studies providing a higher parasite dose pre-turnout followed by natural infection: Höglund et al. (2013) (rows 1 and 2) and Dimander et al. 2003 (rows 3 and 4). Traits shown: body weight (BW), faecal egg count (FEC) in wet faeces, density of L3 on dry herbage, daily feed intake (FI), number of adult worms, and logarithm of the effective reproduction number R_e. The parasite dose at turnout was a 40000 (top) and 10000 (bottom) even mixture of *O. ostertagi* and *C. oncophora*. Results of the statistical tests are given in Table 6.